

# BioCapt® Single-Use

Aktiver Luftkeimsammler

*Testfertiger, aktiver Ersatz für Sedimentationsplatten*



- Kontinuierliche Luftprobenahme und Überwachung
- Testfertiger Ersatz für Sedimentationsplatten
- Weniger Handhabungsschritte und weniger falsch-positive Untersuchungen
- Für den mobilen oder remote Einsatz
- Auswahl verschiedener Agarformulierungen und Flussraten
- Erfüllt ISO 14698-1 und den erwarteten EU-GMP-Annex 1 Einweg-Anforderungen
- Verwendung mit aktiven Luftkeimsammler-Instrumenten für eine vollständig validierte Lösung

Mehr erfahren



**PARTICLE  
MEASURING  
SYSTEMS®**

a spectris company




**Kontaktieren Sie uns für mehr Informationen:**

[www.pmeasuring.de](http://www.pmeasuring.de)

T: +49 351 8896 3850

E: [pmsgermany@pmeasuring.com](mailto:pmsgermany@pmeasuring.com)

# Process intensification strategies toward cell culture-based high-yield production of a fusogenic oncolytic virus

Sven Göbel<sup>1</sup> | Karim E. Jaén<sup>1,2</sup> | Marie Dorn<sup>1,3</sup>  | Victoria Neumeyer<sup>2</sup> | Ingo Jordan<sup>4</sup>  | Volker Sandig<sup>4</sup> | Udo Reichl<sup>1,5</sup> | Jennifer Altomonte<sup>2</sup> | Yvonne Genzel<sup>1</sup> 

<sup>1</sup>Bioprocess Engineering, Max Planck Institute for Dynamics of Complex Technical Systems, Magdeburg, Germany

<sup>2</sup>Department of Internal Medicine II, Klinikum Rechts der Isar, Technische Universität München, München, Germany

<sup>3</sup>Faculty of Process and Systems Engineering, Otto-von-Guericke-University Magdeburg, Magdeburg, Germany

<sup>4</sup>ProBioGen AG, Berlin, Germany

<sup>5</sup>Chair for Bioprocess Engineering, Otto-von-Guericke-University Magdeburg, Magdeburg, Germany

## Correspondence

Yvonne Genzel, Bioprocess Engineering, Max Planck Institute for Dynamics of Complex Technical Systems, Sandtorstr. 1, 39106 Magdeburg, Germany.  
Email: [genzel@mpi-magdeburg.mpg.de](mailto:genzel@mpi-magdeburg.mpg.de)

## Funding information

Max-Planck-Gesellschaft; EXIST

## Abstract

We present a proof-of-concept study for production of a recombinant vesicular stomatitis virus (rVSV)-based fusogenic oncolytic virus (OV), rVSV-Newcastle disease virus (NDV), at high cell densities (HCD). Based on comprehensive experiments in 1 L stirred tank reactors (STRs) in batch mode, first optimization studies at HCD were carried out in semi-perfusion in small-scale cultivations using shake flasks. Further, a perfusion process was established using an acoustic settler for cell retention. Growth, production yields, and process-related impurities were evaluated for three candidate cell lines (AGE1.CR, BHK-21, HEK293SF) infected at densities ranging from 15 to 30 × 10<sup>6</sup> cells/mL. The acoustic settler allowed continuous harvesting of rVSV-NDV with high cell retention efficiencies (above 97%) and infectious virus titers (up to 2.4 × 10<sup>9</sup> TCID<sub>50</sub>/mL), more than 4–100 times higher than for optimized batch processes. No decrease in cell-specific virus yield (CSVY) was observed at HCD, regardless of the cell substrate. Taking into account the accumulated number of virions both from the harvest and bioreactor, a 15–30 fold increased volumetric virus productivity for AGE1.CR and HEK293SF was obtained compared to batch processes performed at the same scale. In contrast to all previous findings, formation of syncytia was observed at HCD for the suspension cells BHK 21 and HEK293SF. Oncolytic potency was not affected compared to production in batch mode. Overall, our study describes promising options for the establishment of perfusion processes for efficient large-scale manufacturing of fusogenic rVSV-NDV at HCD for all three candidate cell lines.

## KEYWORDS

cell culture-based production, fusogenic oncolytic virus, high cell density culture, perfusion, process intensification, upstream processing

**Abbreviations:**  $\mu$ , cell-specific growth rate; CRE, cell retention efficiency; CSPR, cell-specific perfusion rate; CSVY, cell-specific virus yield; CVSPR, cell volume-specific perfusion rate; F, fusion protein; GFP, green fluorescent protein; HCD, high cell density; hpi, hours post infection; IAV, influenza A virus; IC<sub>50</sub>, half maximal inhibitory concentration; IFN, interferon; MOI, multiplicity of infection; NDV, Newcastle disease virus; NS, nutrient supplementation; OV, oncolytic virus; PEM, protein expression medium; rVSV-NDV, recombinant hybrid virus: VSV backbone and surface glycoproteins of NDV used in this study; rVSV-NDV-GFP, recombinant hybrid virus expressing GFP; STR, stirred tank bioreactor; TCID<sub>50</sub>, 50% tissue culture infective dose; TOI, time of infection; VCC, viable cell concentration; VSV, vesicular stomatitis virus; V<sub>w</sub>, working volume; VVP, volumetric virus productivity.

Sven Göbel and Karim E. Jaén contributed equally to this study.

This is an open access article under the terms of the Creative Commons Attribution-NonCommercial-NoDerivs License, which permits use and distribution in any medium, provided the original work is properly cited, the use is non-commercial and no modifications or adaptations are made.

© 2023 The Authors. *Biotechnology and Bioengineering* published by Wiley Periodicals LLC.

## 1 | INTRODUCTION

Cancer poses a high burden on worldwide societal and health care systems, both epidemiologically and financially. Due to a globally aging and still growing human population, cancer is projected to have a significant impact in the coming decades. Cancer immunotherapy is revolutionizing clinical oncology as an exciting paradigm shift by recruiting the patients' immune system against tumors. Originally developed as direct cytotoxic agents, oncolytic viruses (OVs), as therapeutic vaccines, offer an elegant approach to cancer therapy. On the one side, they have the ability to cause direct tumor cell lysis, while on the other side, they can stimulate immune responses directed against the tumor (Cook & Chauhan, 2020; Krabbe & Altomonte, 2018). By expressing endogenous or heterologous fusion glycoproteins, an enhanced intratumoral spread of OVs via syncytia formation can be achieved. The novel engineered recombinant vesicular stomatitis virus-Newcastle disease virus (rVSV-NDV), a recombinant vesicular stomatitis virus (VSV) backbone with fusogenic mutant glycoproteins of NDV, demonstrated preclinical efficacy in various cancer models (Abdullahi et al., 2018; Krabbe et al., 2021).

Manufacturing methods for several oncolytic viruses (herpes simplex virus, vaccinia virus, reovirus, and adenovirus) for clinical trials, but also for rVSV-NDV, are mainly performed in anchorage-dependent cell lines (Abdullahi et al., 2018; Ungerechts et al., 2016). The use of adherent cells can be beneficial due to established and automated production facilities, years of experience with regulatory approval, and high cell-specific virus yields (CSVY) (Pelz et al., 2022). However, for fusogenic OVs that cause formation of large multinucleated syncytia that die rapidly after induction only relatively low virus yields were achieved in several tested adherent cell lines (Abdullahi et al., 2018). This property presents unique challenges for large-scale clinical-grade manufacturing, further compounded as scaling-up of processes for adherent cells is mainly achieved by scaling-out (e.g., increasing the surface area by multiplying the number of culture vessels) or the use of microcarrier systems. In static culture systems, there are also only limited options for monitoring and control of cultivation parameters such as pH values, dissolved oxygen concentration, feeding rates (Gallo-Ramírez et al., 2015; Pelz et al., 2022). Moreover, media for most adherent cells are supplemented with animal-derived components such as fetal calf serum, which can lead to batch-to-batch variations, increased production and purification costs, and elevated contamination risks.

To overcome such limitations, manufacturing can be shifted toward suspension cells using chemically defined media. Suspension cells allow for easy scale-up and passaging while maintaining rapid cell growth. Cultivation in stirred tank bioreactors (STR) can achieve high cell concentration in a small footprint, decreasing labor expenditures (Pelz et al., 2022). Moreover, suspension cultures allow the use of advanced process monitoring methods, enable process automation, and tight control of culture conditions.

As a first step, suitable suspension cell substrates were identified for the development of an efficient and scalable OV production process using a green fluorescent protein (GFP)-expressing variant of rVSV-NDV (rVSV-NDV-GFP). Infection at cell concentrations of about  $2 \times 10^6$  cells/mL yielded titers in the order of  $10^8$  TCID<sub>50</sub>/mL in BHK-21, HEK293SF, and AGE1.CR suspension cells (Göbel, Kortum et al., 2022). However, clinical treatment with OVs will require manufacturing processes that consistently achieve even higher virus titers. Because dose-limiting effects of rVSV-NDV have not been observed in preclinical investigations, processes enabling the production of  $\geq 10^9$ – $10^{10}$  virions/injection are desired. To further increase virus titers in bioreactor harvests, intensification strategies commonly applied in manufacturing of viral vaccines and viral vectors can be adopted. In particular, a switch from batch to perfusion mode and the implementation of high cell density (HCD) processes have been shown as a successful strategy for various virus-host cell systems (Genzel et al., 2014; Gränicher et al., 2021; Lavado-García et al., 2020; Nikolay et al., 2018; Pihl et al., 2018; Vázquez-Ramírez et al., 2018; Wu et al., 2021). Moreover, by adapting feeding schemes after infection (e.g., “hybrid fed-batch/perfusion” [Vázquez-Ramírez et al., 2019]) both CSVY and volumetric virus productivity (VVP) can be further increased compared to perfusion-only strategies. Cell retention devices used to keep cells inside the bioreactor can also influence the performance of production processes (Gränicher et al., 2020). While membrane clogging and accumulation of viruses inside bioreactors are well known drawbacks of membrane-based cell retention (Genzel et al., 2014; Hadpe et al., 2017; Hein, Chawla et al., 2021; Nikolay, Grooth, et al., 2020), both tangential flow filtration (Coronel et al., 2019; Nikolay et al., 2018) and alternating tangential flow filtration (ATF) (Genzel et al., 2014; Gränicher et al., 2020; Gränicher et al., 2021; Hein, Chawla et al., 2021; Vázquez-Ramírez et al., 2019) have been applied successfully in academic research. Effective continuous harvesting of lytic viruses has been demonstrated with devices such as acoustic settlers (Coronel et al., 2020; Gränicher et al., 2020; Gränicher et al., 2021; Henry et al., 2004; Manceur et al., 2017; Petiot & Kamen, 2013). Using an acoustic settler, Gränicher et al. demonstrated an increase of CSVY of at least 1.5-fold through continuous removal of an influenza A virus (IAV) compared to an ATF system (Gränicher et al., 2020). Moreover, by preclarifying the virus-containing harvest for subsequent in-line purification steps, fully integrated virus production processes can be established (Gränicher et al., 2021).

In this study, we investigated process intensification strategies for further improvement of the production of rVSV-NDV in three candidate suspension cell lines. Shake flasks were used as a small-scale screening model in semi-perfusion mode and optimized culture conditions were subsequently transferred to STRs. Acoustic settler perfusion processes in bioreactors using manual and automated perfusion control were established to increase virus titers. Results demonstrate the applicability of perfusion HCD processes for the production of fusogenic oncolytic viruses in suspension cell culture to achieve higher virus titers as well as improved VVP compared to conventional batch production for all candidate cell lines.

## 2 | MATERIALS AND METHODS

### 2.1 | Cell lines, media, and viral seed stock

Three different suspension cell lines (Supporting Information: Table S1) were cultured and screened to identify a suitable cell substrate for the HCD production of rVSV-NDV. AGE1.CR cells were cultivated in chemically defined medium CD-U7 (Xell), supplemented with 2 mM alanine, 2 mM glutamine (Sigma Aldrich), and 10 ng/mL recombinant insulin-growth factor (LONG-R<sup>3</sup>, Sigma-Aldrich). BHK-21 and HEK293SF cells were cultivated in Protein Expression Medium (PEM) (Gibco) supplemented with 8 mM L-glutamine and 4 mM pyruvate (Sigma-Aldrich). All three cell lines were cultivated in baffled 125 mL shake flasks with vent caps (Corning) with a working volume ( $V_w$ ) of 50 mL, and incubated in a Multitron orbitally shaken incubator (Infors AG) with 50 mm shaking diameter. BHK-21 and AGE1.CR cells were incubated at 185 rpm, 37°C, and 5% CO<sub>2</sub>. HEK293SF cells were incubated at 130 rpm, 37°C, and 8% CO<sub>2</sub>. Adherent Huh7 cells were cultivated in T75 flasks (Greiner Bio-one) in high glucose DMEM (Gibco) supplemented with 10% fetal calf serum, 1x nonessential amino acids (Gibco) and 1 mM sodium pyruvate (Gibco) and incubated at 37°C and 5% CO<sub>2</sub>.

For infections, the non-GFP-expressing construct (VSV-NDV) of the previously described rVSV-NDV-GFP (Abdullahi et al., 2018; Göbel, Kortum et al., 2022) was used. Virus stocks were generated from the first passage of rVSV-NDV produced in adherent AGE1.CR-pIX cells (ProBioGen AG) with a titer of  $2.47 \times 10^7$  TCID<sub>50</sub>/mL (rVSV-NDV(pIX)). After subsequent expansion in either AGE1.CR (rVSV-NDV (CR)) or BHK-21 (rVSV-NDV(BHK)) suspension cells, titers of  $5.92 \times 10^5$  TCID<sub>50</sub>/mL and  $1.33 \times 10^9$  TCID<sub>50</sub>/mL, respectively, were achieved. Aliquots of the stocks were stored at -80°C and were used once for each experiment to prevent loss of infectivity due to repeated freeze-thaw cycles. Both preparations were used in experiments. Although enveloped viruses may adapt to a cellular substrate also by incorporation of host cell proteins in their viral envelope we do not expect an impact on production of VSV-NDV: We have not observed significant changes in infectious titers for any cell line and passaging cycle in earlier experiments (Göbel, Kortum et al., 2022), and infection of AGE1.CR, HEK293SF or BHK-21 cells with virus material produced in the respective other cell lines did not significantly affect maximum infectious virus titers (data not shown).

### 2.2 | Small-scale infection studies

For a multiplicity of infection (MOI) screening, HEK293SF cells were inoculated at  $2 \times 10^6$  cells/mL (centrifugation of the appropriate volume at 300g for 5 min; resuspension in 75 mL fresh PEM medium supplemented with 4 mM pyruvate and 8 mM glutamine) in single use 125 mL baffled shake flasks with vent caps (Thermo Fisher Scientific) at 37°C, 8% CO<sub>2</sub> and 130 rpm orbital shaking. Cells were subsequently infected at MOIs of 1E-2–1E-4 at time of infection with rVSV-NDV(CR).

Semi-perfusion was performed by manually exchanging the medium to maintain sufficient metabolite concentrations. For cell growth, a cell-specific perfusion rate (CSPR)-based strategy was used and switched to a strategy based on fixed-reactor volume (RV) after infection as the lytic nature of rVSV-NDV complicated cell count-based feeding strategies. The required exchange volume was calculated according to Vázquez-Ramírez et al. (2018). Cultures were started with a viable cell concentration (VCC) of  $2 \times 10^6$  cells/mL in 50 mL supplemented CD-U7 or PEM medium in single-use 250 mL baffled shake flasks with vented cap (Thermo Fisher Scientific) at the respective cultivation conditions. To avoid potential nutrient limitations, the medium was partially exchanged every 24 h at a CSPR of 50 pL/cell/d for AGE1.CR cells and 83 pL/cell/d for HEK293SF cells targeting for a minimum glucose concentration of 10 mM, respectively, starting at 24 h post inoculation. The calculated cell culture volume was transferred from the shake flasks to 50 mL centrifuge tubes (Greiner Bio One) and centrifuged at 300g for 5 min at room temperature. After removing the supernatant, cells were recovered in an equal volume of fresh medium and transferred back to the shake flasks.

AGE1.CR cells were infected with rVSV-NDV(pIX) in 125 mL baffled shake flasks at a VCC of  $20.0 \times 10^6$  cells/mL following a complete medium exchange. After infection, the manual exchange was paused, and the  $V_w$  was increased from 25 to 50 mL at 12 h post infection (hpi) similar to the process described by Vazquez-Ramírez et al. (2019) and Gränicher et al. (2021) ("Hybrid fed-batch perfusion"). Starting from 24 hpi, a constant perfusion rate of 1.6 RV/d was maintained. A total of six different conditions were investigated as outlined in Table 1.

HEK293SF cells were infected at VCCs of  $10.0 \times 10^6$  and  $20.0 \times 10^6$  cells/mL at a MOI of 1E-3 with rVSV-NDV(CR). Upon infection, medium was exchanged at a fixed perfusion rate of 1.8 RV/d. Medium was further supplemented to yield 35 mM glucose after 96 h, and 35 mM glucose and 12 mM glutamine 144 h post inoculation with the aim to maintain glutamine and glucose concentrations above 4 and 10 mM, respectively.

### 2.3 | Batch cultivations in STR

Bioreactor cultivations were carried out in a 1 L STR (DASGIP, Eppendorf AG). The bioreactors were instrumented with pH (Hamilton) and polarographic pO<sub>2</sub> (Hamilton) probes. Additionally, permittivity probes were used for on-line monitoring of VCC. Cultures were stirred using a pitched blade impeller at 180 rpm (AGE1.CR), 250 rpm (HEK293SF), and 350 rpm (BHK-21). Aeration was carried out through a submerged L-drilled holes sparger at a rate of 3 sL/h. pH value was controlled at 7.2 (AGE1.CR and BHK-21) or 7.0 (HEK293SF) by either sparging CO<sub>2</sub> up to 10% volume or by the addition of 7.5% NaHCO<sub>3</sub> solution. pO<sub>2</sub> was kept equal or above 50% air saturation for the growth phase by sparging O<sub>2</sub> and either 5% air saturation in hypoxic cultivations or equal or above 50% air saturation for the infection phase. Temperature was set at 37°C for

**TABLE 1** Conditions for the hybrid fed-batch perfusion strategy with AGE1.CR cells infected with rVSV-NDV.

Condition	1	2	3	4	5	6
MOI	1E-3	1E-4	1E-5	1E-4	1E-4	1E-4
Temperature pi	37	37	37	34	37	37
Medium	CD-U7	CD-U7	CD-U7	CD-U7	CD-U7/PEM (75:25)	CD-U7 + 1/6 F12

Note: Cells were grown until they reached a density of  $20.0 \times 10^6$  cells/mL (VW = 50 mL). At time of infection (TOI) a complete medium exchange was performed, and the VW was set to 25 mL. Twenty-five milliliter of fresh medium was added once at 12 hpi. Starting at 24 hpi, a constant perfusion rate of 1.6 RV/d was maintained. F12: Ham's Nutrient Mixture F12 (Sigma Aldrich). Temperature in °C.

Abbreviations: MOI, multiplicity of infection; NDV, Newcastle disease virus; pi, post infection; rVSV, recombinant vesicular stomatitis virus.

the growth phase and either 34 or 37°C for the infection phase, and was controlled by means of an electrical heating blanket.

Bioreactors were inoculated at a VCC of  $0.8 \times 10^6$  cells/mL for AGE1.CR and  $0.5 \times 10^6$  cells/mL for BHK-21 and HEK293SF cells, from pre-cultures expanded in 250 mL baffled shake flasks with vented cap (Corning). For the infection phase, an equal  $V_w$  of prewarmed fresh media containing the rVSV-NDV(CR) was transferred to the bioreactor. For the nutrient supplementation (NS) experiments, the infection medium for BHK-21 and HEK293SF cells consisted of PEM supplemented with 60 mM glucose, 17.4 mM glutamine and 8 mM pyruvate. For AGE1.CR cells, CD-U7 medium supplemented as described above was used for infection.

## 2.4 | Perfusion cultivations in STR

Bioreactor perfusion cultivations were carried out in a 1 L STR (DASGIP, Eppendorf AG) (AGE1.CR and BHK-21) and in a 1 L STR Biostat B Plus (Sartorius) (HEK293SF). Cells grew initially in batch mode at 37°C. Cultures were stirred using a pitched blade impeller at 180 rpm. Once they reached a threshold concentration of glucose (5–15 mM), perfusion was started at a rate of 1 RV/d. Subsequently, medium was exchanged on a CSPR basis of 55 pL/cell/d for AGE1.CR, 197 pL/cell/d for HEK293SF, and 110 pL/cell/d for BHK-21 cells. At the STR outlet, cells were retained in a Sono Sep APS-10 acoustic settler (SonoSep Technologies) operated in pump-mode at 3 W and 2.1 Mhz, with backflush every 3 min for 30 s. The feed pump was integrated to the bioreactor weight control system, which comprised a ICS425 scale (Mettler-Toledo) (AGE1.CR and BHK-21) or Midrics 1 (Sartorius) (HEK293SF) to keep a constant weight in the bioreactor during the continuous harvesting performed by a peristaltic pump. For AGE1.CR cells, the permeate flow rate was controlled automatically through a multi-frequency capacitance probe and pre-amplifier (Incyte Hamilton), both connected with a M12 cable to the ArcView controller 265 (Hamilton). The controller was connected to a peristaltic pump (120U, Watson Marlow) by a 4–20 mA output box (Hamilton), with an open-end AUX M12 to the output port of the ArcView and an open-end cable with a 15-pin D-SUB male connector to the pump (Gränicher et al., 2021; Hein, Kollmus et al., 2021; Nikolay, 2020). The cell culture in the bioreactor was monitored in real-time by measuring the permittivity

every 12 min in the range of 0.1–10 MHz. Linear regression between the permittivity signal and the VCC was used to determine a “cell factor” of 0.67 which was stored in the ArcView controller to set the cell volume-specific perfusion rate (CVSPR) of  $0.04 \text{ pL}/\mu\text{m}^3/\text{d}$  for AGE1.CR cells. For BHK-21 and HEK293SF cells, the CSPR was adjusted manually by increasing the pump once a day based on off-line VCC and metabolite measurements.

Cells were recirculated by a peristaltic pump (Watson Marlow 120U, UK) through a 5 mm inner diameter silicon tubing, operated at 3–5 RV/d. For the infection phase, a volume of medium of 50 mL containing the rVSV-NDV was transferred to the bioreactor. HEK293SF cells were infected with rVSV-NDV(BHK) with a MOI of 1E-3, BHK-21 cells with rVSV-NDV(BHK) with a MOI of 1E-4, and AGE1.CR cells with rVSV-NDV(BHK) with a MOI of 1E-5. After infection, the temperature was shifted to 34°C, the recirculation rate was increased to 5 RV/d for all cell lines, and the perfusion rate was set at 3 RV/d for HEK293SF cells. For AGE1.CR and BHK-21 cells, the previously described “hybrid fed-batch” strategy was pursued, which consisted of a 1:1.8 dilution by addition of fresh medium at 12 hpi and subsequent exchange with 2 RV/d starting 24 hpi. All the cultures were performed in a  $V_w$  of 400–600 mL at pH 7.2 and at  $pO_2$  equal or above 50% air saturation during the entire cultivation time. The overall setup including devices for control of perfusion is shown in Figure 1.

## 2.5 | Oncolytic viral potency assay

The half maximal inhibitory concentration (IC<sub>50</sub>) potency assay determines the MOI of VSV-NDV, which results in 50% cell killing at a defined time point, as a quantitative parameter to compare the relative potency of VSV-NDV-mediated cytotoxicity derived from the different production cell lines. Huh7 cells were seeded one day before infection at a density of  $1.0 \times 10^4$  cells/well in an opaque-walled flat-bottom 96-well plate in DMEM. After overnight incubation, cells were infected in half-log steps from MOI 1E1 to MOI 1E-4 with VSV-NDV produced in perfusion cultures from BHK-21, AGE1.CR or HEK293SF cells. At 48 hpi, cell viability was measured using the CellTiter-Glo Assay (Promega) according to the manufacturer's instructions, and luminescence was measured using the Promega GloMax Plate Reader (Promega). For the analysis of IC<sub>50</sub> values, GraphPad PRISM software (GraphPad Software Inc) was used. Briefly, viability data was

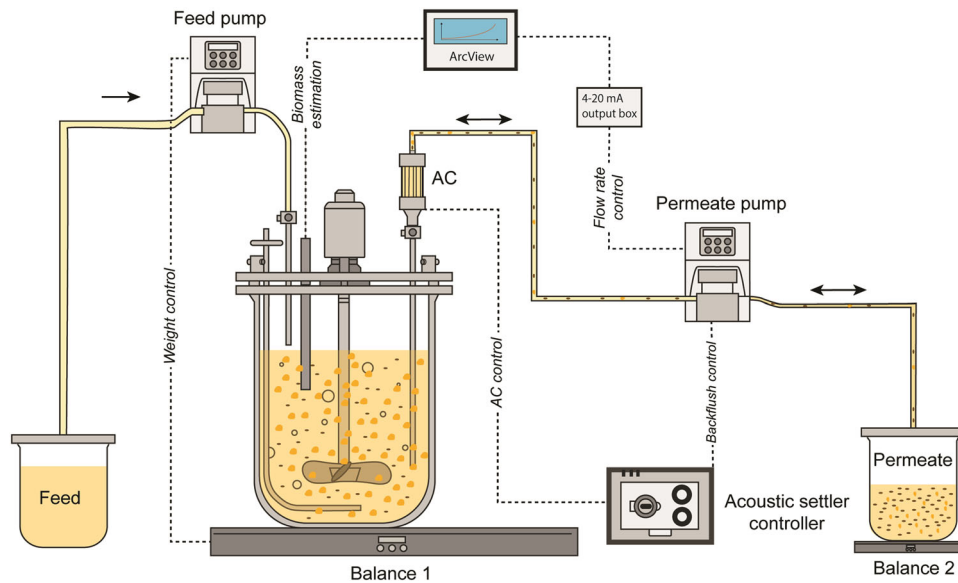


**FIGURE 1** Scheme of the acoustic settler setup for perfusion cultivations (adapted from [Göbel, Pelz et al., 2022]). Cell retention was achieved by generation of a standing wave field in the APS-10 acoustic settler (AC) chamber. For AGE1.CR cell cultivations, viable cell volume was monitored on-line using a capacitance probe and used to maintain the cell volume-specific perfusion rate at a steady state during the cell growth phase. Permeate flow rates were confirmed by using balance 2. As separation depended strongly on the cell diameter, viable cells were retained while dead cells were washed out into the permeate. Virus particles, not effected by the generated wave field, were collected in the permeate vessel. Orange circles indicate cells, orange dots indicate cell debris, black ellipses indicate virus particles, and dashed lines indicate different types of signal transmissions.

normalized to untreated controls and data was transformed. Then, IC50 values were calculated by nonlinear regression curve fitting using a log (agonist) versus normalized response (variable slope) curve fit.

## 2.6 | Other analytics

Samples from cultures were collected every 24 h during growth phase and every 12 h during the infection phase. Samples of 1 mL were used for pH and osmolality measurements, and cell counting to determine the VCC, cell viability and cell diameter in a ViCell-XR (Beckman Coulter). Off-line pH was measured in a pH7110 potentiometer (Inolab). Osmolality was measured in a vapor pressure osmometer VAPRO 5600 (Wescor, Inc). Samples of 1 mL for virus titration, metabolite and impurity measurements were centrifuged at 1100g for 5 min. The supernatant was recovered and distributed in 500  $\mu$ L aliquots in 2 mL cryovials stored at  $-80^{\circ}\text{C}$  until further analysis. Metabolite concentrations (glucose, lactate, glutamine, glutamate, and ammonium) were determined using a Bioprofile 100 (Nova Biomedical). For titration of VSV-NDV, the previously described TCID<sub>50</sub> assay (Göbel, Kortum et al., 2022) was performed using adherent AGE1.CR. pIX cells. The CSVY was calculated as previously described by Gränicher et al. (2020) taking into account only the error of the TCID<sub>50</sub> assay ( $-50\%/+100\%$  on a linear scale).

To determine the amount of impurities (protein and DNA), the methodology of Marichal-Gallardo et al. (2017) was used. Supernatant samples were dialyzed in PBS buffer at  $2-8^{\circ}\text{C}$  for at least 16 h, using 14 kDa MWCO cellulose acetate membranes (Spectrum). Protein

concentrations were quantified using the colorimetric BCA assay according to the manufacturer's instructions (Thermo Fischer Scientific). After incubation at  $37^{\circ}\text{C}$  for 30 min, the absorbance was measured in an Infinite M200 plate reader (Tecan) at 562 nm. Protein concentrations were obtained after relating absorbance measurements from the standard calibration curve. A pico-green fluorescence-based assay was used to quantify the concentration of double stranded host cell DNA (dsDNA). Briefly, 200  $\mu$ L of the blank (PBS), lambda DNA standards and dialyzed samples were loaded in duplicate in a 96-flat bottom black multi-well plate. After addition of 50  $\mu$ L of 1:60 pico-green solution, the plate was incubated and shaken at room temperature and 1000 rpm for 5 min in a Thermomixer Comfort (Eppendorf). The fluorescence was read in a Tecan M200 Pro (Tecan) at 480 nm (excitation)/520 nm (emission). DNA concentrations were obtained after relating fluorescence measurements from a standard calibration curve.

Purification of virus was performed using ultracentrifugation and a sucrose gradient. Briefly, medium containing viral particles was obtained and virus was pelleted by ultracentrifugation at 65,000 rcf for 1 h at  $4^{\circ}\text{C}$ . Viral particles were purified via ultracentrifugation over a sucrose gradient and the pellet was resuspended in phosphate-buffered saline (PBS) after an additional ultracentrifugation step.

Computation of the TCID<sub>50</sub> was carried out according to the Reed and Muench method (Rammanikhrisan 2016). The stoichiometric lactate to glucose yield ( $Y_{\text{Lac/Glc}}$ ), the total number of accumulated virus particles ( $\text{vir}_{\text{tot}}$ ), the CSVY, the VVP and the accumulated mass of dsDNA and protein (Prot) were calculated as described by Gränicher et al. (2020); as follows:

$$Y_{Lac/Glc} = \frac{(C_{Lac,n} - C_{Lac,n-1}) + 0.5 \times (C_{Lac} + C_{Lac,n-1}) \times \frac{V_p}{V_w}}{(C_{Glc,n-1} - C_{Glc,n}) + (C_{Glc,0} - 0.5 \times (C_{Glc} + C_{Glc,n-1})) \times \frac{V_p}{V_w}} \quad (1)$$

$$vir_{tot} = C_{vir,STR} \cdot V_w + \sum 0.5 \times (C_{vir,H,n} + C_{vir,H,n-1}) \times V_H \quad (2)$$

$$CSVY = \frac{vir_{tot}}{X_{v,STR,max} \times V_w} \quad (3)$$

$$VVP = \frac{vir_{tot}}{V_{tot} \times t_{tot}} \quad (4)$$

$$dsDNA = C_{dsDNA,Br} \times V_w + \sum 0.5 \times (C_{dsDNA,H,n} + C_{dsDNA,H,n-1}) \times V_H \quad (5)$$

$$Prot = C_{Prot,tot,Br} \times V_w + \sum 0.5 \times (C_{Prot,tot,H,n} + C_{Prot,tot,H,n-1}) \times V_H \quad (6)$$

where  $C_{Lac,n}$  is the lactate concentration at time  $n$  ( $t_n$ ) (mM),  $V_p$  is the perfused volume between  $t_n$  and  $t_{n-1}$ , and  $C_{Glc,0}$  and  $C_{Glc,n}$  is the glucose concentration at time 0 and  $n$ , respectively.  $vir_{total}$  is the total number of accumulated infectious viral particles (TCID<sub>50</sub>),  $C_{vir,STR}$ ,  $C_{vir,H,n}$ , and  $C_{vir,H,n-1}$  (TCID<sub>50</sub>/mL) are the infectious virus concentrations in the bioreactor and the harvests at  $t_n$  and  $t_{n-1}$ , respectively.  $V_H$  is the volume harvested between  $t_n$  and  $t_{n-1}$  (mL).  $X_{v,STR,max}$  (cells/mL) is the maximum viable cell concentration upon infection in the bioreactor,  $V_{tot}$  is the total medium spent including cell growth phase,  $t_{tot}$  is the total process time from inoculation until the time point of maximum  $vir_{tot}$ .  $C_{dsDNA,STR}$ ,  $C_{dsDNA,H,n}$ , and  $C_{dsDNA,H,n-1}$  (μg/mL) are the concentrations of double stranded DNA in the bioreactor and the harvests at  $t_n$  and  $t_{n-1}$ , respectively. Finally,  $C_{Prot,STR}$ ,  $C_{Prot,H,n}$ , and  $C_{Prot,H,n-1}$  (μg/mL) are the concentrations of protein in the bioreactor and the harvests at  $t_n$  and  $t_{n-1}$ , respectively.

The cell retention efficiency of the acoustic settler (CRE) (%) was calculated as follows:

$$CRE = \left(1 - \frac{X_{v,H}}{X_{v,Br}}\right) \times 100, \quad (7)$$

Where  $X_{v,H}$  and  $X_{v,STR}$  are the viable cell concentrations in the harvest and in the bioreactor, respectively.

### 3 | RESULTS

We previously identified three promising suspension cell lines (AGE1.CR, HEK293SF, BHK-21) for the batch production of rVSV-NDV-GFP in shake flasks and STRs (Göbel, Kortum et al., 2022). To confirm that the reported process parameters would still be applicable for the production of rVSV-NDV (same construct but without the GFP reporter gene for use in clinical studies) shake flask experiments were performed. This included infections using the optimal MOIs identified. Here, no significant differences were found (data not shown).

#### 3.1 | rVSV-NDV production in STR in batch mode

Previously, the use of a STR resulted in slightly lower TCID<sub>50</sub>/mL titers for BHK-21 cells and drastically reduced titers for HEK293SF cells (Göbel, Kortum et al., 2022). Therefore, the impact of nutrient supplementation (NS) on the rVSV-NDV production was now additionally evaluated for BHK-21 and HEK293SF cells, respectively. Moreover, the effect of a temperature shift (34°C) (BHK-21), hypoxia (pO<sub>2</sub> 5%) and trypsin addition (5 U/mL) (HEK293SF) on the infection phase were investigated (Figure 2).

During the growth phase, AGE1.CR cells grew exponentially at a specific rate of 0.018 1/h with a viability above 90%. Once a VCC of about  $4.0 \times 10^6$  cells/mL was reached, a  $V_w$  of freshly supplemented CD-U7 medium containing the rVSV-NDV(pIX) virus was added to the bioreactor to infect the cells at a MOI of 1E-5. At 36 hpi, cell viability was below 90% and a maximum infectious virus titer of  $7.50 \times 10^5$  TCID<sub>50</sub>/mL (Figure 2d) and CSVY of 0.3 TCID<sub>50</sub>/cell were reached. Addition of nutrient-enriched medium at time of infection (TOI) for BHK-21 cells maintained glucose and glutamine concentrations above 15 and 2 mM, respectively (Supporting Information: Figure S1). This did not influence the cell growth (Figure 2b), but resulted in a two-fold increase in the maximum infectious virus titer (Figure 2e) and the CSVY. Shifting the temperature to 34°C after infection, neither affected cell growth nor the maximum infectious virus titer (Figure 2b,e) and CSVY compared to the cultivation performed at 37°C. For HEK293SF cells, increasing the glucose (60 mM) and glutamine (17 mM) concentrations in the infection medium restored the concentration of both substrates at the levels observed upon inoculation (Supporting Information: Figure S1). In all conditions, cells first grew exponentially from  $2.0 \times 10^6$  to  $5.4 \times 10^6$  cells/mL within 48 hpi but cell concentrations stagnated for the rest of the cultivation (Figure 2c). Cell viability slightly declined from 48 hpi onwards, but remained above 90% until 120 hpi (Figure 2c). rVSV-NDV production was barely increased by nutrient supplementation (Figure 2f). In comparison to the rVSV-NDV-GFP infection at MOI 1E-2 (Figure 2c,f reference) with a maximum titer of  $1.0 \times 10^6$  TCID<sub>50</sub>/mL, infections with rVSV-NDV(CR) at MOI 1E-3 resulted in titers lower than  $1 \times 10^6$  TCID<sub>50</sub>/mL but an up to four-fold increase in CSVY. However, these subtle improvements were suppressed under hypoxia, where the infectious virus titer was similar to the reference (Figure 2c,f) but with a 50% lower CSVY. Trypsin addition led to a 30% increase in maximum infectious virus titer (Figure 2f) and CSVY. Overall, it seems that overcoming substrate limitations was pivotal to improve rVSV-NDV production in 1 L STR cultures (Table 2).

#### 3.2 | Medium switch and transition to semi-perfusion mode for AGE1.CR cells

As for HEK293SF cells, the maximum infectious virus titer for AGE1.CR cells was decreased by more than one order of magnitude after transfer from shake flask cultivations (Figure 2) to STR operated in batch mode. Two strategies were followed to increase the maximum virus titers:

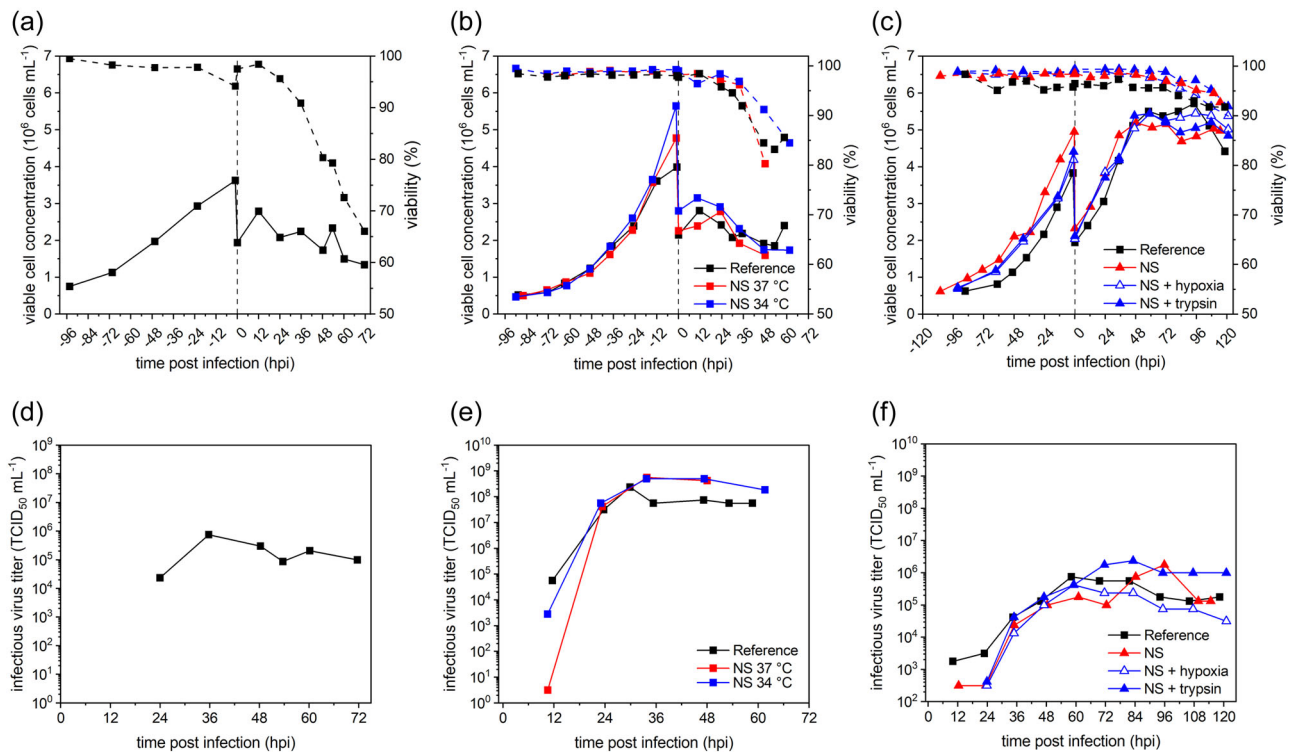


**FIGURE 2** rVSV-NDV production in candidate cell lines in 1 L STR in batch mode. rVSV-NDV production in AGE1.CR cells (a, d); Influence of nutrient supplementation (NS) and temperature shift to 34°C on rVSV-NDV production in BHK-21 cells (b, e), and hypoxia (pO<sub>2</sub> 5%) and trypsin addition (5 U/mL) on rVSV-NDV production in HEK293SF cells (c, f), in 1 L STR cultures in batch mode. All cultures were infected at 2 × 10<sup>6</sup> cells/mL following a 1:2 dilution step with fresh medium. (a–c) Viable cell concentration (solid lines) and viability (dashed lines), (d–f) infectious virus titer. Reference refers to the data obtained from Göbel, Kortum et al. (2022) with the rVSV-NDV-GFP construct (37°C without NS). NDV, Newcastle disease virus; rVSV, recombinant vesicular stomatitis virus; STR, stirred tank bioreactors.

**TABLE 2** Growth and rVSV-NDV production in 1 L STR cultures in batch mode with three candidate cell lines.

Cell line	Condition	MOI (virus)	pO <sub>2</sub> (%)	$\mu$ (h <sup>-1</sup> )	Max. VCC p.i (×10 <sup>6</sup> cell mL <sup>-1</sup> )	Max. infec. virus titer (TCID <sub>50</sub> mL <sup>-1</sup> )	Time of max. titer (hpi)	CSVY (TCID <sub>50</sub> /cell)	VVP (×10 <sup>8</sup> TCID <sub>50</sub> /L/d)
AGE1.CR	37°C	1E-5 (pIX)	≥50	0.018	2.79	7.50 × 10 <sup>5</sup>	36.0	0.3	1.2
BHK-21	Reference	1E-4 (pIX)	≥50	0.027	2.81	2.37 × 10 <sup>8</sup>	29.8	84.0	480
BHK-21	NS 37°C	1E-4 (CR)	≥50	0.028	2.79	5.62 × 10 <sup>8</sup>	33.8	202.0	1126
BHK-21	NS 34°C	1E-4 (CR)	≥50	0.033	3.16 ± 0.25	5.01 × 10 <sup>8</sup> ± 8.70 × 10 <sup>7</sup>	33.8 ± 0.1	161.0 ± 40	937 ± 266
HEK293SF	Reference	1E-2 (pIX)	≥50	0.027	5.72	7.50 × 10 <sup>5</sup>	45.8	0.1	1.4
HEK293SF	NS	1E-3 (CR)	≥50	0.020	5.20	1.78 × 10 <sup>6</sup>	95.8	0.3	2.1
HEK293SF	NS + hypoxia	1E-3 (CR)	5	0.019	5.45	4.22 × 10 <sup>5</sup>	59.1	0.1	0.6
HEK293SF	NS + trypsin	1E-4 (CR)	≥50	0.020	5.45	2.37 × 10 <sup>6</sup>	83.2	0.4	3.2

Note: Reference refers to the data obtained from Göbel, Kortum et al. (2022) with the rVSV-NDV-GFP construct (37°C, without NS). CR and pIX refer to the previously described cell source used for production of the stock virus. BHK-21 NS 34°C cultures are reported as the mean and standard deviation of two independent STR cultivations.

Abbreviations: CSVY, cell-specific virus yield; NS, nutrient supplementation; p.i., post infection; VVP, volumetric virus productivity; ≥, equal or greater than.

1. Exchange to PEM medium at TOI, as high virus titers for both HEK293SF and BHK-21 cells were achieved in PEM medium in shake flasks, respectively.
2. Transfer to semi-perfusion to mimic lab-scale perfusion processes and achieve HCD.

We previously reported a rapid decrease of infectious virus titer in AGE1.CR cells in CD-U7 medium in shake flasks for the rVSV-NDV-GFP construct (Göbel, Kortum et al., 2022). Although the infectious virus titer of rVSV-NDV was stable in STR batch cultivations for AGE1.CR cells (see Section 4.1), a similar degradation kinetic was observed in shake flask



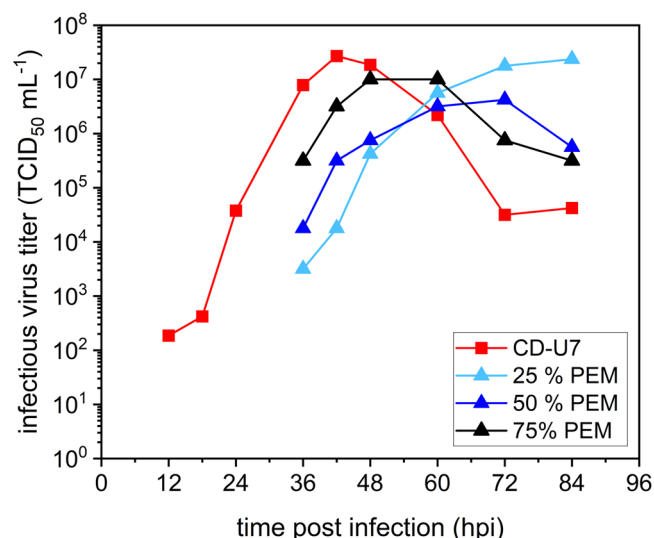


**FIGURE 3** Effect of medium replacement at time of infection on virus stability at time of infection for rVSV-NDV production in AGE1.CR cells. AGE1.CR cells were grown in baffled 125 mL shake flasks ( $V_w = 50$  mL, 185 rpm) and infected at a viable cell concentration of  $2.0 \times 10^6$  cells/mL with rVSV-NDV(pIX) at a MOI of  $1E-5$ . At time of infection, the growth medium was removed completely and exchanged to the respective CD-U7/PEM mixtures. NDV, Newcastle disease virus; rVSV, recombinant vesicular stomatitis virus.

cultivations (Figure 3). On the other hand, infectious virus titers remained stable in PEM medium used for cultivation of BHK-21 and HEK293SF cells, although strong declines in viability were observed. Our initial hypothesis was that CD-U7 medium, as opposed to PEM medium, was lacking a compound that could prevent virus degradation. To evaluate the potential of a medium exchange at TOI for AGE1.CR cells, various media with CD-U7/PEM ratios ranging from 25% to 75% were tested in shake flask cultivations (Figure 3).

Addition of PEM medium at time of infection did not result in an increase of the maximum infectious virus titer compared to the infection carried out with CD-U7 medium, regardless of the ratio. However, as shown in Figure 3, ratio-dependent changes in virus dynamics could be observed: While the maximum infectious virus titer in CD-U7 media was reached 42 hpi, a slower replication kinetic was observed for all PEM contents. Here, the maximum infectious virus titer was reached faster with increasing PEM contents, 84i, 72, and 48 hpi for 25%, 50%, and 75%, respectively. Interestingly, a strong reductions of infectious virus titers could be prevented for a PEM content of 25% within 84 hpi. However, viability of all PEM spiked cultures stayed above 90% over the entire infection period, while it decreased to 50% at 60 hpi for CD-U7 (data not shown).

A commonly applied strategy to overcome nutrient limitations and the accumulation of inhibitors is the transition from batch mode to perfusion. Here, fresh media is added constantly, while spent medium is simultaneously removed. As higher cell concentrations can be reached in perfusion mode, overall higher virus titers and VVPs can be attained if the CSVY is kept constant. As for now, rVSV-NDV was not investigated in high cell density cultivations above  $10.0 \times 10^6$  cells/mL. Therefore, a

semi-perfusion strategy was evaluated in shake flasks to achieve higher cell concentrations ( $>20.0 \times 10^6$  cells/mL) to optimize process conditions for subsequent bioreactor processes in perfusion mode. Several parameters that can influence the virus production were varied: temperature at time of infection, media composition and MOI (Table 1). For six different conditions (C1-C6), a MOI screening with MOIs  $1E-3$  –  $1E-5$ , a temperature shift to  $34^\circ\text{C}$ , and two different media compositions, were investigated.

During cell propagation, CD-U7 medium was used for C1–C5, whereas for C6 a mixture of CD-U7 and F12 medium (6:1) was used. For all conditions, cells grew without a noticeable lag-phase with an average  $\mu$  of 0.024 1/h (Figure 4d). With the initiation of the semi-perfusion mode 48 h after inoculation, the metabolite concentrations started to stabilize at levels between 15 and 25 mM for glucose, 10–20 mM for lactate, 1.5 mM for glutamine, and 0.5 mM for ammonium (data not shown). After a complete medium exchange at TOI, the cells continued to grow until 18–36 hpi (Figure 4). Shortly thereafter, the cell viability started to decline and dropped below 80% at 48 hpi for C1–C3. After the complete medium exchange, the metabolite concentrations reached a stable level at 12 hpi, which was maintained with feeding and the re-start of the semi-perfusion mode until the end of the cultivations (data not shown).

For all conditions, except for C3, the start of infectious virus production was observable at 12–18 hpi. As shown in Figure 4a, higher MOIs did not result in higher infectious virus titers although maximum values were reached earlier. For C1 and C2, virus production peaked at 36 hpi with maximum titers of  $1.0 \times 10^6$  TCID<sub>50</sub>/mL and  $1.3 \times 10^6$  TCID<sub>50</sub>/mL before decreasing until the end of the cultivation. In comparison, the maximum infectious virus titers reached with a MOI of  $1E-5$  (C3) were increased by more than one order of magnitude compared to the higher MOI. However, the infectious virus titer declined faster (by 1 log within 12 h) after reaching the maximum value (Figure 4a). Shifting the temperature to  $34^\circ\text{C}$  after infection (C4) resulted in a 3-fold increase of maximum infectious virus titer at a MOI of  $1E-4$ . Titters of C3 continued to increase until 42 hpi peaking at a maximum of  $4.2 \times 10^6$  TCID<sub>50</sub>/mL before slowly declining until the end of the process. Interestingly, the decrease in temperature was not able to slow down the degradation of infectious virus particles (Figure 4b). Lastly, two different media compositions with supplementation of CDU7 with PEM medium (C5) and F12 medium (C6) were tested (Figure 4c). For both conditions, the infectious virus titers increased exponentially and maximum values of  $5.6 \times 10^6$  TCID<sub>50</sub>/mL at 42 hpi (C6) and  $3.2 \times 10^7$  TCID<sub>50</sub>/mL at 48 hpi (C5) were achieved, respectively (Figure 4c). This corresponded to a 20-fold (PEM) and 4-fold (F12) increase in maximum infectious virus titers compared to the cultivation with CD-U7 base medium (C2) (Table 3). Nevertheless, neither supplementation with PEM nor addition of F12 medium were able to prevent virus degradation after the maximum titer was reached (Figure 4c). When comparing the maximum accumulated infectious virus titers of the best conditions (C3 and C5), an increase was achieved by supplementing PEM medium compared to C3. Regardless of the strategy used, the CSVY was significantly

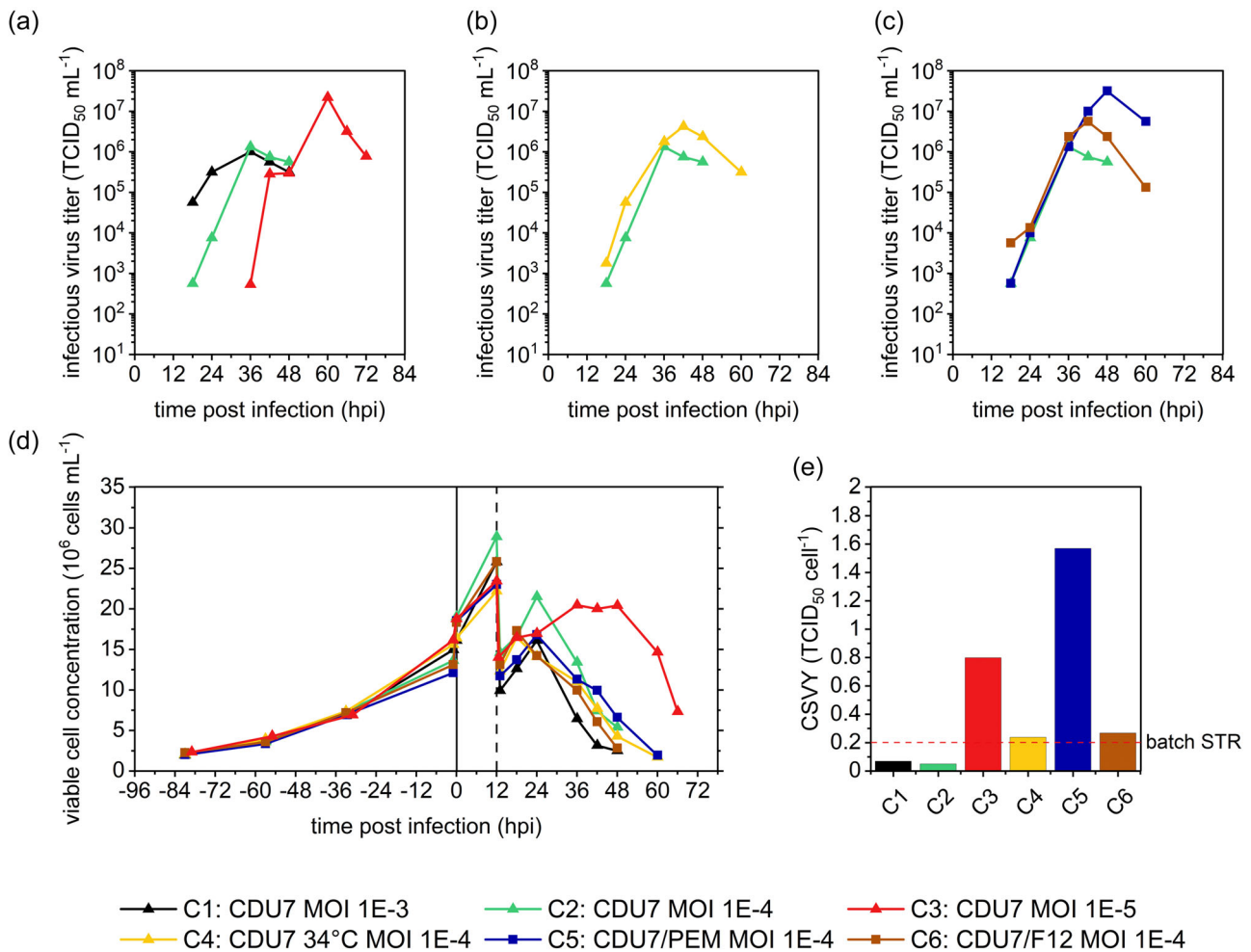


**FIGURE 4** Infectious virus titers, cell growth and CSVY for AGE1.CR cells infected with rVSV-NDV(pIX) in semi-perfusion mode in shake flasks. AGE1.CR cells were grown to high cell concentrations (HCD) in 125 mL shake flasks ( $V_w = 50$  mL) in semi-perfusion mode and infected at  $20 \times 10^6$  cells/mL after a complete medium exchange. Fresh medium was added at 12 hpi (two-fold dilution; dashed line). C1–C3 were infected with MOIs ranging from  $1E-3$  to  $1E-5$  and continuously maintained in CD-U7 medium at  $37^\circ\text{C}$ . Similarly, C4–C6 were infected with a MOI of  $1E-4$ , but parameters were modified. For C4, the temperature was decreased to  $34^\circ\text{C}$  after infection, while for C5 the medium was changed to a mixture of 75% CDU7% and 25% PEM. Cells of C6 were continuously maintained in CDU7/F12 (6:1) at  $37^\circ\text{C}$ . Semi-perfusion with 1.6 RV/d was restarted 24 hpi, where 80% of the culture supernatant was exchanged 36, 48, and 60 hpi. (a–c) infectious VSV-NDV titer for (a) MOI screening at HCD, (b) temperature shift  $37^\circ\text{C}$  to  $34^\circ\text{C}$  at HCD, (c) medium composition at HCD, (d) cell growth, (e) CSVY. CSVY, cell-specific virus yield; NDV, Newcastle disease virus; rVSV, recombinant vesicular stomatitis virus.

decreased compared to shake flask cultivations in batch mode. Nevertheless, compared to the batch cultivation in the STR (Table 2), a more than five-fold increase in CSVY was achieved for C5. Moreover, the VVP was 200-fold higher for C5 compared to the batch cultivation in the STR, suggesting a benefit of HCD cultivations not only for increasing virus titers but also for reducing medium consumption (Table 3).

### 3.3 | High cell density production of rVSV-NDV in HEK293SF cells in semi-perfusion mode

In the preceding experiments, we were able to confirm the potential of semi-perfusion culture for the production of rVSV-

NDV. Therefore, infection cell concentrations of  $10.0 \times 10^6$  and  $20.0 \times 10^6$  cells/mL were evaluated for HEK293SF cells in a next step. Upon infection, VCC increased to  $25.2 \times 10^6$  and  $26.8 \times 10^6$  cells/mL with viabilities above 90%, respectively (Figure 5a). From 72 hpi onwards, cell viability rapidly declined. Interestingly, growth of cells infected at higher cell concentrations was significantly slower although optimal metabolite levels were maintained throughout the infection phase (Supporting Information: Figure S2). Nevertheless, maximum titers up to  $8.0 \times 10^7$  TCID<sub>50</sub>/mL were achieved in both cultures around 84–96 hpi (Figure 5b). Semi-perfusion cultures either infected at  $10.0 \times 10^6$  or  $20.0 \times 10^6$  cells/mL displayed no differences in either maximum titers ( $4.2 \times 10^7$ – $1.0 \times 10^8$  TCID<sub>50</sub>/mL) (Figure 5b) or CSVY (Table 3), also if compared against shake

**TABLE 3** Cell growth and rVSV-NDV production in the shake flask cultures of AGE1.CR and HEK293SF cells in semi-perfusion mode.

Cell line	Condition	MOI (virus)	$\mu$ ( $\text{h}^{-1}$ )	Max. VCC p.i ( $\times 10^6$ cell $\text{mL}^{-1}$ )	Max. infec. virus titer ( $\text{TCID}_{50}$ $\text{mL}^{-1}$ )	Time of max. titer (hpi)	CSVY ( $\text{TCID}_{50}/\text{cell}$ )	VVP ( $\times 10^8$ $\text{TCID}_{50}/\text{L}/\text{d}$ )
AGE1.CR	C1	1E-3 (pIX)	0.026	16.1	$1.0 \times 10^6$	36	0.01	1.6
AGE1.CR	C2	1E-4 (pIX)	0.024	21.5	$1.3 \times 10^6$	36	0.01	1.3
AGE1.CR	C3	1E-5 (pIX)	0.025	21.3	$2.3 \times 10^7$	60	0.10	10.8
AGE1.CR	C4	1E-4 (pIX)	0.026	14.1	$4.2 \times 10^6$	42	0.05	3.5
AGE1.CR	C5	1E-4 (pIX)	0.023	16.8	$3.2 \times 10^7$	48	1.60	22.0
AGE1.CR	C6	1E-4 (pIX)	0.022	14.2	$5.6 \times 10^6$	42	0.06	4.0
HEK293SF	$10 \times 10^6$ cells/mL	1E-3 (CR)	0.023	$25.2 \pm 1.4$	$1.0 \times 10^8$	$78 \pm 9$	$11 \pm 1$	$20.5 \pm 2.4$
HEK293SF	$20 \times 10^6$ cells/mL	1E-3 (CR)	$0.027 \pm 0.001$	$26.8 \pm 3.3$	$7.1 \times 10^7 \pm 4.1 \times 10^7$	$84 \pm 17$	$7 \pm 2$	$11.0 \pm 4.6$

Note: All maximum cell concentrations are normalized to the highest dilution applied after infection at 12 hpi. CR and pIX refer to the previously described cell source used for production of the stock virus. Results for HEK293SF cells are reported as the mean and standard deviation of two independent shake flask cultivations. CSVY: cell-specific virus yield, p.i: post infection, VVP: volumetric virus productivity.

Abbreviations: CSVY, cell-specific virus yield; NDV, Newcastle disease virus; pi, post infection; rVSV, recombinant vesicular stomatitis virus; VVP, volumetric virus productivity.

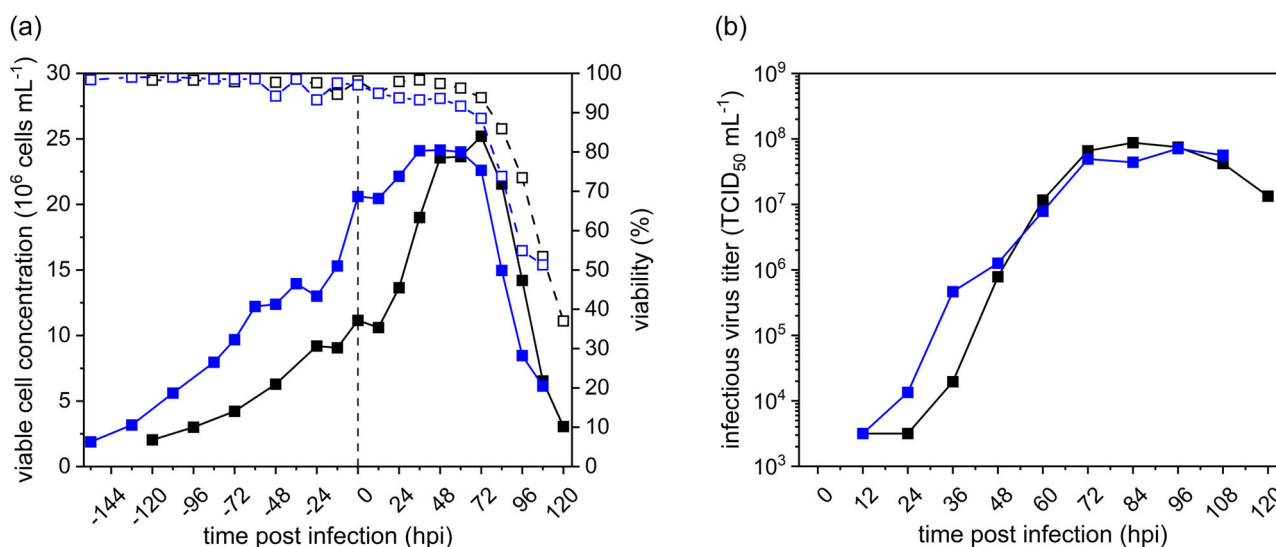


**FIGURE 5** Effect of cell density at time of infection on rVSV-NDV production in HEK293SF cells in semi-perfusion cultures in shake flasks. (a) Viable cell concentration (solid lines) and viability (dash lines and open symbols) during growth and virus production of HEK293SF cells infected at viable cell concentrations of  $10.0 \times 10^6$  cells/mL (black) and  $20.0 \times 10^6$  cells/mL (blue), respectively; (b) infectious virus titer of cells infected at viable cell concentrations of (black)  $10.0 \times 10^6$  cells/mL and (blue)  $20.0 \times 10^6$  cells/mL, respectively. Values are reported as the mean of a biological duplicate of two independent shake flasks. NDV, Newcastle disease virus; rVSV, recombinant vesicular stomatitis virus.

flask batch cultures infected at  $2.0 \times 10^6$  cells/mL (data not shown).

Nevertheless, there were benefits in terms of virus production by doubling the infection cell concentration. Compared to the batch STR run (Table 2), a 36-fold increase in CSVY was achieved for cells infected at  $10.0 \times 10^6$  cells/mL, indicating a possible advantage of a semi-perfusion strategy for rVSV-NDV production. Additionally, the VVP was up to 6-fold higher in comparison to the highest VVP achieved in the 1 L STR, which exemplifies that higher productivities could be achieved at lower  $V_w$ .

### 3.4 | Process intensification in STRs using perfusion mode

Finally, cultivations of AGE1.CR, BHK-21 and HEK293SF cells were carried out in perfusion mode using a 1 L STR and an acoustic settler as cell retention device. A cell concentration of  $30.0 \times 10^6$  cells/mL was targeted for AGE1.CR and BHK-21 cells at TOI using the DASGIP STR system. In contrast, based on results obtained in semi-perfusion mode in shake flasks, HEK293SF cells were infected at lower cell concentrations of  $15.0 \times 10^6$  cells/mL in the Biostat B STR system. All cell lines displayed viabilities exceeding 95% and consistent growth during the exponential

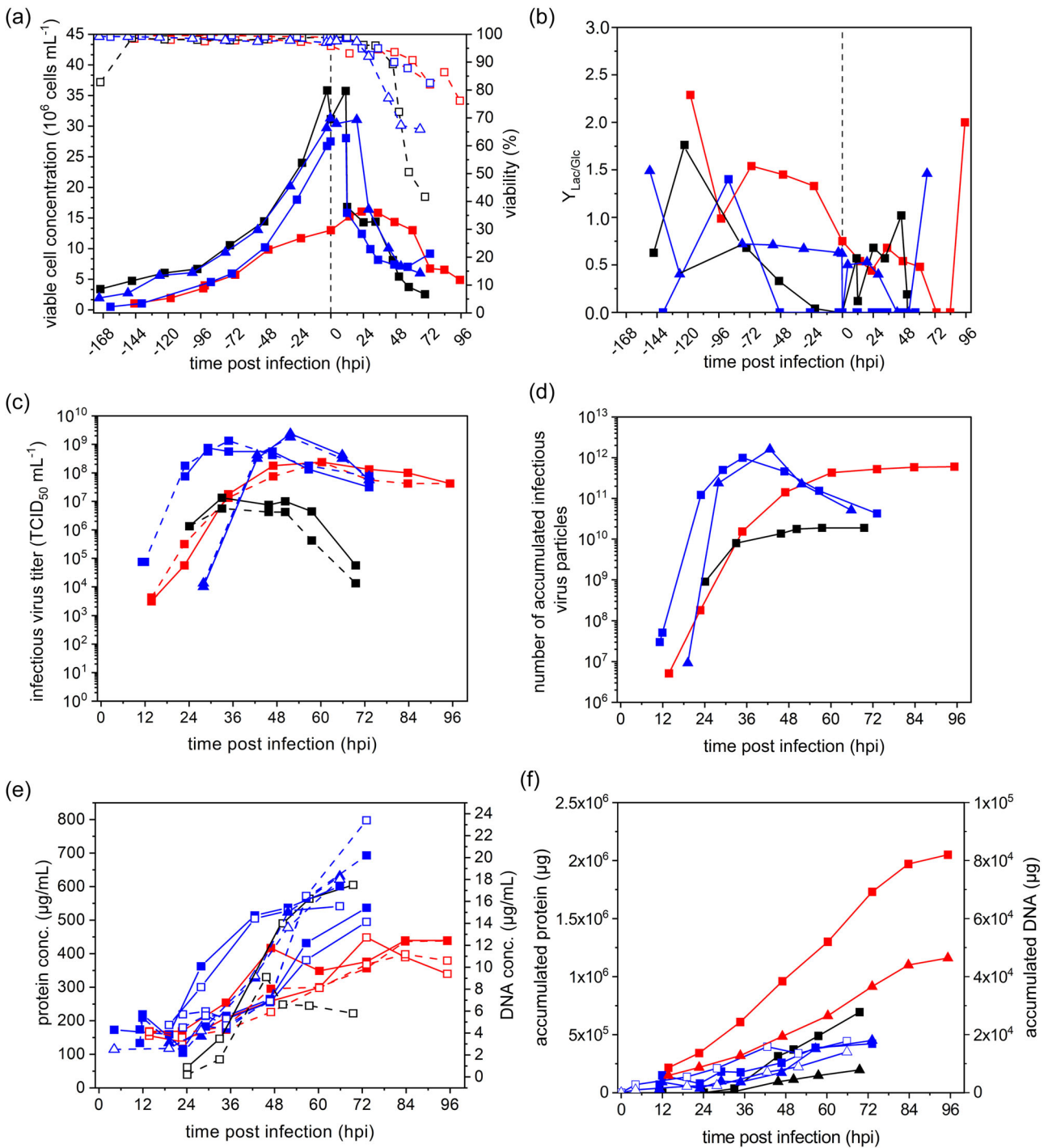


**FIGURE 6** rVSV-NDV production in AGE1.CR (black), BHK-21 (blue), and HEK293SF (red) cells in 1 L STR cultures in perfusion mode using an acoustic settler for cell retention. (a) Viable cell concentration (solid lines) and viability (dashed lines and open squares), (b)  $Y_{\text{Lac/Glc}}$  yield, (c) infectious virus titer in the bioreactor (dashed lines) and in the harvest (solid lines) fractions, (d) accumulated number of infectious virus particles, (e) concentration of protein (solid line) and DNA (dashed line) in the bioreactor (filled squares) and in the harvests (empty squares), and (f) accumulated total protein (squares) and host cell DNA (triangles). AGE1.CR and BHK-21 cells were cultivated in a DASGIP system, HEK293SF cells were cultivated in a Biostat system. BHK-21 cultivation II data is shown in triangles in (a–e), and as empty symbols in (f). NDV, Newcastle disease virus; rVSV, recombinant vesicular stomatitis virus.

growth phase. HEK293SF cells grew exponentially in batch mode with  $\mu = 0.024$  1/h during 48 h, reaching  $3.2 \times 10^6$  viable cells/mL. Cells continued growing under perfusion with  $\mu = 0.018$  1/h, and within 96 h reached  $12.0 \times 10^6$  viable cells/mL with a viability above 95%. Upon

infection, cells had a brief growth period of 24 h reaching a maximum VCC of  $16.0 \times 10^6$  cells/mL (Figure 6a). During batch mode, AGE1.CR cells grew slowly with  $\mu = 0.012$  1/h reaching  $6.7 \times 10^6$  cells/mL. After initiation of perfusion, cells expanded exponentially with  $\mu = 0.018$  1/h

**TABLE 4** Cell growth and rVSV-NDV production in 1 L STR cultures in perfusion mode.

Cell line	Condition	MOI (virus)	$\mu$ ( $\text{h}^{-1}$ )	Max. VCC p.i ( $\times 10^6$ cell $\text{mL}^{-1}$ )	Max. infec. virus titer (TCID <sub>50</sub> $\text{mL}^{-1}$ )	Time of max. titer (hpi)	CSVY (TCID <sub>50</sub> /cell)	VVP ( $\times 10^8$ TCID <sub>50</sub> /L/d)
AGE1.CR	Hybrid FB	1E-5(BHK)	0.016	[31.15] 16.80	$1.3 \times 10^7$	33.0	1.5	3.8
BHK-21Cultivation I	Hybrid FB	1E-4(BHK)	0.022	[28.05] 15.85	$7.5 \times 10^8$	29.2	110	428.0
BHK-21Cultivation II	Hybrid FB	1E-4(BHK)	0.017	[31.40] 16.40	$2.4 \times 10^9$	42.6	126	343.0
HEK293SF	Perfusion	1E-3(BHK)	0.018	[13.00] 16.05	$2.4 \times 10^8$	60.2	75	49.3

Note: Maximum viable cell concentrations are given at time of infection [] and during infection. (BHK) refers to the previously described cell source used for production of the stock virus.

Abbreviations: CSVY, cell-specific virus yield; FB, fed-batch; NDV, Newcastle disease virus; pi, post infection; rVSV, recombinant vesicular stomatitis virus; VVP, volumetric virus productivity.

reaching  $35.0 \times 10^6$  cells/mL within 96 h (Figure 6a). The fact that specific growth rates were similar to batch cultivations in bioreactors for HEK293SF and AGE1.CR cells (Table 2) suggests that cell growth was not impaired by high cell concentrations and use of the acoustic settler. For BHK-21 cells,  $\mu$  was in the range 0.025–0.030 1/h during batch mode. After initiation of perfusion,  $\mu$  dropped to 0.020 and 0.014  $\text{h}^{-1}$  but cell concentration continued to increase to 28.5–31.0  $\times 10^6$  cells/mL, respectively for both replicates (Figure 6a). For all cultivations, a cell retention efficiency above 97% was achieved during cell growth phase using the acoustic settler (Supporting Information: Figure S4).

Glucose and glutamine concentrations were above 10 and 3 mM, respectively, over the entire cultivation period for all cell lines. Lactate accumulated to maximum concentrations of 28 mM for HEK293SF, 18 mM for BHK-21 and 12 mM for AGE1.CR cells during batch mode, and decreased to about 20 mM for HEK293SF, 13 mM for BHK-21, and 2 mM for AGE1.CR cells during perfusion. Ammonium and glutamate concentrations were below 1.5 and 3 mM, respectively, over the entire cultivation period for all cell lines (Supporting Information: Figure S3). pH value and osmolality were 7.0–7.6 and 250–340 mOsmol/Kg for all cultures, respectively (Supporting Information: Figure S4).

To assess the metabolic performance of the cells, the lactate to glucose yield ( $Y_{\text{Lac/Glc}}$ ), was calculated. Maximum values of the  $Y_{\text{Lac/Glc}}$  were reached predominantly during the growth phase in batch mode. The  $Y_{\text{Lac/Glc}}$  was stabilized during the growth phase in perfusion mode at values around 1.5 mmol lactate/mmol glucose for HEK293SF cells, 0.25 mmol lactate/mmol glucose for BHK-21 cells, and 0 mmol lactate/mmol glucose for AGE1.CR cells. Upon infection, the  $Y_{\text{Lac/Glc}}$  exhibited an abrupt increase for all cell lines, particularly toward the end of the cultivations, to levels close to that observed during growth in batch mode.

As mentioned before, higher cell concentrations can lead to increased amounts of nonquantified substrates and virus production inhibitors, which can decrease the CSVY and virus titers. Mammalian cell growth requires at least 13 amino acids (Eagle, 1959). Therefore, to avoid limitations of nonquantified metabolites, cell culture medium was additionally exchanged with a high flow-rate (5 RV/d) 2 h before infection. This high exchange rate resulted in a 14% loss of cells for the AGE1.CR cultivation through the acoustic chamber (Figure 6a).

By reducing the maximum flow rate to 4 RV/d, a retention efficiency of 99% was achieved for BHK-21 and HEK293SF cells, respectively (Supporting Information: Figure S4).

Overall, a maximum infectious virus titer of  $2.4 \times 10^8$  TCID<sub>50</sub>/mL for HEK293SF,  $1.3 \times 10^7$  TCID<sub>50</sub>/mL for AGE1.CR and  $7.5 \times 10^8$ – $2.4 \times 10^9$  TCID<sub>50</sub>/mL for BHK-21 cell cultivations was achieved 36–60 hpi in bioreactors (Table 4). As expected, infectious virus titers from bioreactor and harvest vessel samples were practically the same for all cultivations. AGE1.CR and BHK-21 cells continued to grow until 12 hpi in batch mode before being subsequently diluted with fresh medium. HEK293SF cells continued to grow until 24 hpi, after which VCC and viability steadily decreased until the end of the experiment to about 33% of the maximum VCC and 75% viability, respectively (Figure 6a). CSVYs of 75 TCID<sub>50</sub>/cell for HEK293SF, 1.5 TCID<sub>50</sub>/cell for AGE1.CR and 110–126 TCID<sub>50</sub>/cell for BHK-21 cells were obtained in perfusion mode (Table 4). This corresponded to a 250-fold and 1.5-fold increase for HEK293SF and AGE1.CR cells, respectively. For BHK-21 cells no difference was found compared to the best results obtained in batch mode (Table 2). An exchange rate of 2–3 RV/d was sufficient to prevent any limitations in glucose concentrations, and—most likely—the accumulation of inhibitors (Supporting Information: Figure S3). The VVP in perfusion mode was equal to  $3.8 \times 10^8$  TCID<sub>50</sub>/L/d for AGE1.CR,  $4.9 \times 10^9$  TCID<sub>50</sub>/L/d for HEK293SF, and  $3.4$ – $4.3 \times 10^{10}$  TCID<sub>50</sub>/L/d for BHK-21 cells, which was around 15–30-fold higher for AGE1.CR and HEK293SF cells compared to batch processes performed at the same scale (Table 4). For BHK-21 cells, the VVP was 3-fold lower in perfusion mode compared to the batch process (Table 2). Interestingly, the VVP was reduced by 6-fold for AGE1.CR cells when comparing semi-perfusion in shake flasks to perfusion cultivations in STR, although the permeate flow was controlled tightly in the latter. This was not the case for HEK293SF cell cultivations, for which the switch from semi-perfusion to perfusion mode yielded a 2-fold increase in VVP.

To assess the potential burden of high cell concentrations on performance of subsequent downstream purification trains, DNA and total protein levels in the bioreactor and the harvest vessel were determined. During the first 24 hpi, the protein concentration was about 150–200  $\mu\text{g/mL}$  and then began rising in both the bioreactor and harvest vessel for all cell lines (Figure 6e). Samples from the bioreactor displayed slightly higher protein concentrations than

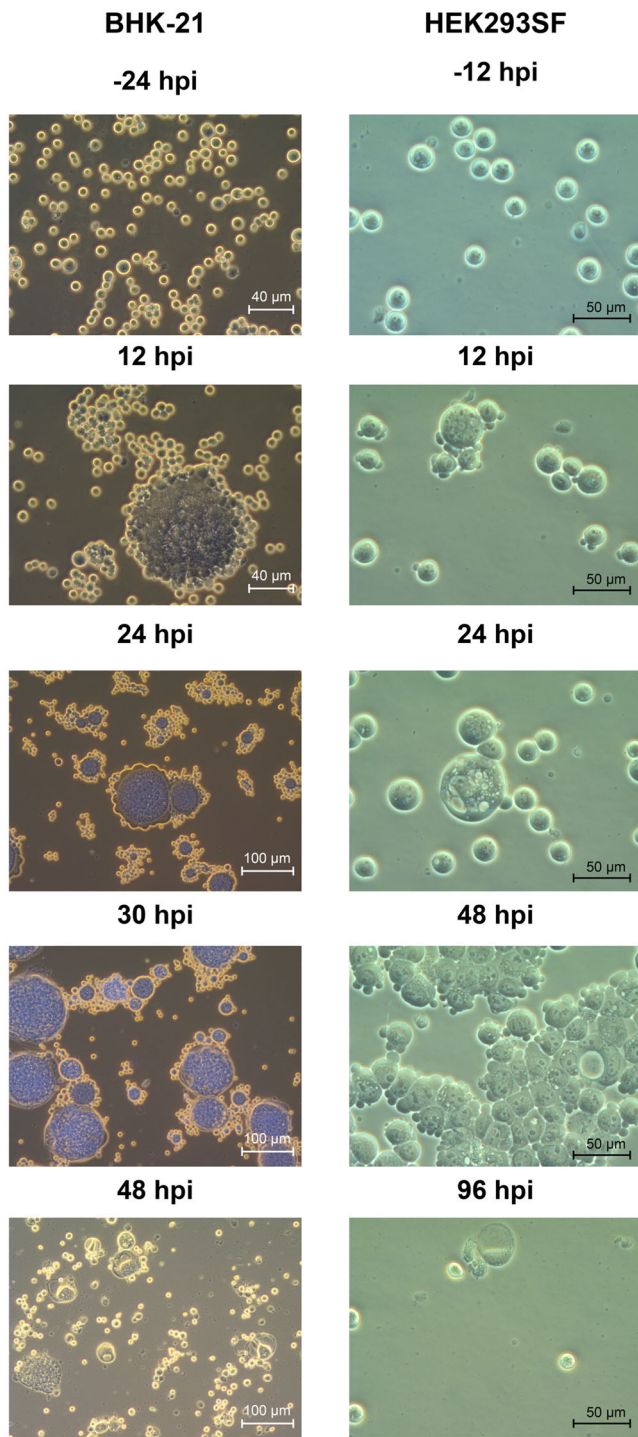


**FIGURE 7** Syncytia formation during rVSV-NDV production in 1 L STR perfusion cultures of BHK-21 and HEK293SF cells. Starting 12 hpi, clusters of fused and enlarged cells appeared in the STR and they lysed after 48 hpi for BHK-21 and 96 hpi for HEK293SF. AGE1.CR did not form syncytia in perfusion culture (not shown). NDV, Newcastle disease virus; rVSV, recombinant vesicular stomatitis virus.

samples from the harvest vessel until about 60 hpi, and reached about 450  $\mu\text{g}/\text{mL}$  at the end of the experiment for HEK293SF cells. Maximum protein concentrations of 600  $\mu\text{g}/\text{mL}$  were reached for BHK-21 and AGE1.CR cells, respectively. The level of DNA began

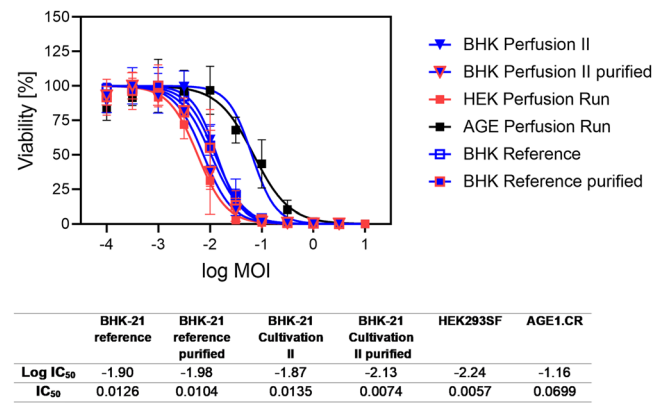


**FIGURE 8** Oncolytic viral potency values for rVSV-NDV produced in perfusion mode. Viability of Huh7 cancer cells was determined 48 hpi with rVSV-NDV generated in the respective suspension cell line grown in perfusion mode and compared to virus generated in BHK-21 cells cultivated in STR in batch mode. Sucrose-gradient purified material of the reference STR batch culture as well as BHK II perfusion culture was additionally included. IC<sub>50</sub> and log IC<sub>50</sub> values determined from the dose-response curves after nonlinear regression analysis. Values are reported as the mean of technical triplicates, with  $n = 3$  for all samples. NDV, Newcastle disease virus; rVSV, recombinant vesicular stomatitis virus.

accumulating from 36 hpi from 4 up to 12  $\mu\text{g}/\text{mL}$  for HEK293SF and AGE1.CR cells, and 18–23  $\mu\text{g}/\text{mL}$  for BHK-21 cells, respectively (Figure 6e). Taking into account the total volume harvested after infection, virus material produced in the HEK293SF cell cultivation had the highest levels of DNA and protein (Figure 6f), approximately four to six-fold higher than for the other cell lines.

In our previous study we found no evidence of syncytia formation in various suspension cell sources, even when inducing cell clumping via supplementation of  $\text{CaCl}_2$  (Göbel, Kortum et al., 2022). Monitoring bioreactor samples by bright-field microscopy confirmed this finding for AGE1.CR cells. No syncytia formation was observed for any time point post infection. Surprisingly, syncytia formation was found for BHK-21 and HEK293 perfusion cultures. Here, clusters of fused and enlarged cells appeared within the first 12 hpi (Figure 7). These clusters reached sizes from 70 to 80  $\mu\text{m}$  in HEK293 to 100–120  $\mu\text{m}$  in BHK-21 cells.

Finally, we investigated whether the production rVSV-NDV at HCD or syncytia formation in perfusion mode has an impact on its oncolytic properties in susceptible Huh7 cells using the IC<sub>50</sub> potency assay. Samples from all STR perfusion cultures were compared to material previously produced in BHK-21 suspension cells in STR culture (Table 2 NS 34°C). Additionally, sucrose-gradient purified material of the reference culture as well as BHK perfusion culture II was tested, to investigate the potential effect of contaminants at HCD on oncolytic potency.

As indicated in Figure 8, rVSV-NDV harvested from the perfusion cultures of HEK293SF cells and BHK-21 run II cell cultures had a similar oncolytic potential in Huh7 cells as the BHK-21 cell reference. Interestingly, the dose required to induce 50% cancer cell

cytotoxicity was 0.7 log higher for rVSV-NDV produced in AGE1.CR cells. Overall, regardless of the cell line, perfusion mode and HCD cultivations did not alter the ability of the produced virus to induce oncolysis. Purification via sucrose-gradient reduced the dose required to induce 50% cancer cell cytotoxicity regardless of the cultivation mode. However, a greater increase in potency was achieved for material produced in perfusion mode.

## 4 | DISCUSSION

Due to the significant advances in oncolytic virotherapy, more and more production modalities are required for clinical studies and applications. To our knowledge, advanced HCD cell culture technologies have not yet been reported for production of clinical grade oncolytic herpes simplex virus, vaccinia virus, and reovirus, (Ungerechts et al., 2016). Among the few descriptions for manufacture at HCD, Grein et al. studied production of oncolytic measles virus in Vero cells attached to microcarriers (Grein et al., 2019). An oncolytic adenovirus was produced in tumor suspension-adapted cells in perfusion cultures in ATF mode (Yuk et al., 2004). Both studies had the goal to achieve a high number of doses containing the up to  $10^{11}$  infectious virus particles per dose that are required for clinical efficacy. Compared to traditional OVs, OV vector platforms that induce syncytia formation in infected cells pose additional challenges to the manufacturing process. In our previous study, we identified several suspension cell substrates that are able to support the replication of the fusogenic rVSV-NDV to high titers in batch mode (Göbel, Kortum, et al., 2022). This study aimed to establish an improved rVSV-NDV manufacturing process for generating high titer stocks from HCD suspension cultures optimizing cell culture medium formulation and infection conditions.

### 4.1 | rVSV-NDV production in STR in batch mode

HEK293 is a well-known host cell line for the production of viral vectors and recombinant proteins (Abaandou et al., 2021; Dumont et al., 2016; Venereo-Sanchez et al., 2016), and has also been explored for the manufacturing of vaccines (Le Ru et al., 2010). HEK-293 cultures are also fully permissive for rVSV-NDV (Göbel, Kortum et al., 2022). However, only low virus titers were obtained in a scale-up from shake flask to 1 L STR in batch mode. To overcome this limitation, several strategies were applied. The first one consisted in a medium supplementation with glucose and glutamine. Providing an optimal metabolic state with a sufficient supply of extracellular substrates is critical to achieve high virus yields (Aunins, 2003). The increase in concentration of these major sources of carbon and energy metabolism doubled rVSV-NDV titers. In addition, a reduction in oxygen partial pressure to 5%  $pO_2$  during virus replication (hypoxia) was considered. Exposing adherent Vero cells to low oxygen levels increased production yields for VSV (Lim et al., 1999). rVSV-NDV is an RNA virus that is highly sensitive to antiviral actions of type I interferons (IFN) (Abdullahi et al., 2018). We previously reported a slow, gradual, and incomplete infection of HEK293SF cells even at higher

MOIs (Göbel, Kortum et al., 2022). Continuously increasing the population of infected cells without losing the cell source due to oncolysis appears favorable if a shift to an antiviral state by IFN signaling cascades can be prevented. Therefore, virus replication was expected to be enhanced if cellular defenses against viral infections mediated by IFN can be inactivated by oxygen limitation (Miar et al., 2020). Trypsin addition was tested along nutrient supplementation to promote virus entry into the cell by hemagglutinin cleavage as required for the production of influenza A virus (Klenk et al., 1975). Trypsin addition has also enhanced influenza A virus replication by proteolytic degradation of IFN (Seitz et al., 2012). While both measures allowed only a modest increase in rVSV-NDV titers (0.5 log), cell growth was not compromised. With the current data a potential accumulation of nonquantified compounds inhibiting viral vector replication cannot be excluded. Such an effect was suggested by the results obtained for BHK-21 cells, where adjustments in medium formulation yielded a doubling of the rVSV-NDV titers and CSVY. A reduction of temperature at time of infection was often found to increase virion stability and/or maximum virus titers (Elahi et al., 2019; Genzel & Reichl, 2009; Kaptein et al., 1997; Nikolay et al., 2018; Petiot et al., 2011; Wechuck et al., 2002). However, in our case, a reduction of temperature to 34°C after infection had neither an effect on cell growth nor on virus stability, maximum infectious virus titer or CSVY. Similar results were obtained for AGE1.CR cells. Overall, we suspect a limitation of nonquantified metabolites or an accumulation of inhibiting molecules to be the reason for this drastic reduction in viral vector titers in comparison to the titers achieved in shake flasks with complete medium exchange at TOI. In a subsequent study, the impact of pH-drifts, as observed in shake flask cultivations, and of differences in shear forces between STR and shake flasks on maximum infectious virus titers could be further investigated.

### 4.2 | Medium switch and transition to semi-perfusion mode for AGE1.CR cells

A rapid decline of infectious activity was observed for both rVSV-NDV (Figure 3) and, previously, for rVSV-NDV-GFP (Göbel, Kortum et al., 2022) in studies with AGE1.CR cultures. To improve titers and virion stability, we investigated an alteration of medium properties at the time of infection (Jordan et al., 2011, 2016). Supplementation of PEM to CD-U7 medium improved viability of AGE1.CR cells for the entire infection period. Although maximum titers did not increase, the level of infectious units were best maintained in cultures with CD-U7 medium containing 25% PEM. We suspect that recombinant insulin, trace elements, or polyamines in PEM could be responsible for improved infectious stability. Hydrolysates are an important component of many serum-free media that can increase buffering capacity and delay cell death so that production intervals are prolonged (Ho et al., 2021). However, CD-U7 does not and (to our knowledge) PEM may also not contain hydrolysates. Polyamines are contained in different ratios and configurations in various advanced and basal media (such as putrescine in F12). They have pleiotropic effects that can support or interfere with viral replication (Mounce et al., 2017). Insulin and insulin-like growth factors have been

demonstrated to inhibit apoptosis in CHO cells (Adamson & Walum, 2007; Ghafari-Esfahani et al., 2020; Sunstrom et al., 2000). Prolonged cell survival may not only increase production of recombinant protein (Ghafari-Esfahani et al., 2020) but may also help in infected cultures to replenish virions lost to degradation. Insulin was furthermore identified as a strong activator of the PI3K/Akt pathway supporting early entry uptake, viral RNA expression, and inhibition of premature apoptosis after IAV infection (Planz, 2013). However, there are also reports discussing contrary results such as a delayed viral replication of IAV or fowl plague virus at low MOIs following insulin supplementation (Scholtissek et al., 1986). For hepatitis B virus in a human hepatoma cell line (Gripon et al., 1989), and for hepatitis A virus in PLC/PRF/5 cells (Gauss-Müller & Deinhardt, 1984) reduced titers reported in media with low insulin concentrations compared to cultivations with media containing other supplements or no supplementation. In summary, as observed here, mixtures of media with different levels of supplementation with factors such as polyamines, insulin and insulin-like growth factor may exhibit complex effects on the kinetic of virus replication and maintenance of infectious units.

In a second step, a semi-perfusion strategy was evaluated in shake flasks to achieve higher cell concentrations ( $>20.0 \times 10^6$  cells/mL) and optimize process conditions for subsequent bioreactor processes performed in perfusion mode. Multiple studies demonstrated increased MVA and IAV virus titers and VVP by applying hybrid perfusion strategies (hybrid fed-batch) after infection (Gränicher et al., 2021; Vázquez-Ramírez et al., 2019). Compared to shake flask cultivations in batch mode, HCD cultivations often resulted in a drastically reduced CSVY. This so-called cell density effect has been shown for a variety of virus production processes (Bock et al., 2011; Ferreira et al., 2007; Kamen & Henry, 2004; Nadeau & Kamen, 2003; Perrin et al., 1995; Tapia et al., 2016; Wood et al., 1982). In this study, no nutrient limitation was observed for any of the investigated cultivations. Also, cultivation at HCD did not require an adaptation of the MOI (Figure 4a). However, by decreasing the temperature after infection to 34°C (C4) and additional supplementation with F12 medium (C6), higher infectious virus titers and CSVYs were obtained for AGE1.CR cells compared to 37°C. Furthermore, addition of PEM to CD-U7 medium (C5) after infection of AGE1.CR cells resulted in yet higher infectious virus titers and CSVYs above 1.5 TCID<sub>50</sub>/cell, although a nonoptimal MOI of 1E-4 was used. Compared to the batch STR cultivation (Table 2), both CSVY and VVP were drastically increased by transition to semi-perfusion at HCD (Table 3).

### 4.3 | High cell density production of rVSV-NDV in HEK293SF cells in semi-perfusion mode

Although HEK293 cells are being used for production of viral vaccines and viral vectors for over 30 years, production at HCD remains impacted by reductions of CSVYs with increasing cell concentrations. This cell density effect is thoroughly described in the literature for a variety of viruses, particularly for adenovirus (Gálvez et al., 2012; Kamen & Henry, 2004; Nadeau & Kamen, 2003),

but also IAV (Petiot & Kamen, 2013), retroviruses (Rodrigues et al., 2013), and virus-like particles (Fontana et al., 2014). Here, infections at concentrations of  $10.0 \times 10^6$  and  $20.0 \times 10^6$  cells/mL did not result in a reduction of CSVY compared to batch cultivations ( $2.0 \times 10^6$  cells/mL), neither in shake flasks nor in STRs. However, there was no benefit in terms of VVP, virus titer or CSVY by increasing the infection cell concentration to  $20.0 \times 10^6$  cells/mL. Although the CSVY in the  $20.0 \times 10^6$  cells/mL infected cultivation at TOI was slightly lower compared to the  $10.0 \times 10^6$  cells/mL infected cultivation at TOI, the difference is negligible and can therefore not be classified as a cell density effect. For these reasons, a concentration below  $20.0 \times 10^6$  cells/mL at TOI was considered as optimal to further investigate rVSV-NDV production in perfusion applications.

For HEK293SF cells, periodically exchanging the medium with a fixed rate of 1.8 RV/d seemed to be sufficient to avoid the aforementioned accumulation or depletion of nonquantified compounds causing a drastic loss of viral vector productivity in STRs. This was also described by Henry et al., who observed increasing CSVYs with increasing perfusion rates for HEK293 for the production of adenoviral vectors using an acoustic settler for perfusion (Henry et al., 2004). Here, compared to cultivation in batch mode in STRs, CSVY was increased by 36-fold, and VVP was up to six-fold, proving this approach to be valuable both for increasing virus titers but also reducing media consumption.

### 4.4 | Process intensification in STRs with perfusion mode

Based on the positive results obtained for rVSV-NDV production in semi-perfusion mode, cultivation of all three candidate cell lines in a STR operated in perfusion mode was evaluated. In the systems tested, a HCD above  $10 \times 10^6$  cells/mL was achieved for all three cell lines. For AGE1.CR cells, cultivation up to  $50.0 \times 10^6$  cells/mL (Genzel et al., 2014) in perfusion mode employing an ATF system was described previously. HEK293SF cells have been grown up to  $15.0 \times 10^6$  cells/mL in perfusion mode using an acoustic settler (Petiot et al., 2011). For a process involving other HEK293 cells, up to  $80.0 \times 10^6$  cells/mL were reached (Schwarz et al., 2020). For BHK-21 cultures, up to  $6.0 \times 10^6$  cells/mL in perfusion mode using a spin filter for the production of rabies virus (Perrin et al., 1995) was obtained; in semi-perfusion mode even up to  $60.0 \times 10^6$  cells/mL were reached (Nikolay, 2020).

Uptake rates for glucose and glutamine for HEK293SF and BHK-21 cells during the cell growth phase were higher than for AGE1.CR cells and consequently a higher CSPR of 197 and 110 pL/cell/d for HEK293SF and BHK-21 cells was needed to maintain sufficient metabolite levels. For comparison, AGE1.CR cells were able to utilize a lower CSPR of 55 pL/cell/d, which was in the same range as shown in previous studies (Gränicher et al., 2021; Vázquez-Ramírez et al., 2018, 2019). Control of the perfusion rate using a capacitance probe allowed a robust process control with stable CSPR values over the entire growth phase (Supporting Information: Figure S4d). Similar



findings were reported for a variety of other cell lines, further underlining the versatility of this method (Gränicher et al., 2021; Hein, Kollmus et al., 2021; Nikolay et al., 2018; Wu et al., 2021).

The  $Y_{\text{Lac/Glc}}$  provides an insight on the glucose usage. Remarkably, HEK293SF cells exhibited higher  $Y_{\text{Lac/Glc}}$  values compared to the other cell lines, beyond 2 mmol lactate/mmol glucose, consistent with previous findings (Petiot et al., 2015). Upon infection, an additional decrease in  $Y_{\text{Lac/Glc}}$  was also observed mainly for HEK293SF cells. The observed shifts may be due to a combination of an increased perfusion rate and from a metabolic redirection caused by the infection process, in which more carbon is channeled to the tricarboxylic acid cycle instead of being converted to lactate with the concomitant NADH oxidation (Petiot et al., 2011, 2015). As observed by Gränicher et al. (2020), the  $Y_{\text{Lac/Glc}}$  of AGE1.CR.pIX cells in perfusion cultures using ATF and acoustic settlers also increased toward the end of the cultivation and coincided with the loss of cell viability. Due to the fusogenic potential of the rVSV-NDV, the acoustic filter was chosen as retention device to avoid possible clogging of membranes in ATF or TFF applications. To address low virus stability, direct harvesting during cultivation was implemented. The acoustic settler in this work was operated in pump recirculation mode that previously was demonstrated to deliver higher virus productivities than valve recirculation mode (Gränicher et al., 2020). As expected, infectious virus titers of the bioreactor and the harvest vessel were similar and allowed accumulation of infectious virus particles above  $10^{11}$  TCID<sub>50</sub> in HEK293SF and BHK-21 cultures. Virus production was considerably improved in comparison to the batch cultures. Although for BHK-21 cells the difference was minimal, they showed in all cultivations the highest CSVY and VVP making BHK-21 the best producer host from the productivity point of view. Possibly, direct cooling of the harvested material could further improve virus stability and thereby increase virus yield. This however, was not tested in the current study.

Regarding the accumulation of impurities, levels of total protein and dsDNA were within the same order of magnitude as reported by Gränicher et al. (2020) for a HCD MVA production process in AGE1.CR.pIX cells. While concentrations of total protein and dsDNA were low for HEK293SF in comparison to BHK-21 cells, accumulated levels of impurities of HEK293SF cells were highest. This is especially surprising as the maximum concentration of HEK293SF cells was much lower than for the other cell lines.

Whether syncytia formation of BHK-21 and HEK293 cells but not of AGE1.CR cells had an effect on the production of the rVSV-NDV remains open. High VCC after infection in AGE1.CR cells would support this phenomenon, but there was no evidence of syncytia formation at low cell concentrations even after induction of aggregation with CaCl<sub>2</sub> (Göbel, Kortum et al., 2022). Particle sizes of the syncytia were in the range of 70–120 μm. Their formation might cause fluid dynamic stress and cell losses due to syncytia-sycytia and syncytia-impeller impacts (Nienow, 2021). While cell retention without a physical barrier (acoustic or inclined settlers and centrifuges) was demonstrated to be efficient, such a requirement introduces new challenges compared to the currently preferred

membrane-based systems (ATF and TFF). Small lumen sizes of hollow-fiber membranes are likely to prevent passage of syncytia, potentially leading to a faster blocking of fibers. On the other side, the use of membrane-based systems could potentially prevent syncytia formation and, therefore, facilitate scale-up of manufacturing processes. In this context, the use of novel membrane systems such as the TDFD from Repligen with large lumen sizes could be an interesting approach for future investigations.

Finally, selective replication, OV spreading and lysis of cancer cells are attributes that need to be considered for production of OVs. This was assessed through a potency assay (EMA, 2009). The scope of the potency measurement was to determine whether cultivation at HCD affected the ability of the virus to induce oncolysis. As crude harvests produced at HCD contain more contaminants (proteins, DNA etc.) than crude material produced in batch culture which are likely to interfere with infectivity and thus potency, increased potency values after purification can be expected. Therefore, a comparison between crude harvest and purified material harvested from the second perfusion cultivation in BHK-21 was carried out and included in the measurement. For a fair comparison, purified material should be used for all perfusion samples, however this was outside of the scope of this study. As demonstrated, for all cell lines, the rVSV-NDV material produced in perfusion mode and at HCD (with and without syncytia formation) was able to induce adequate oncolysis. Compared to material produced in batch mode, the oncolytic potency of material produced in AGE1.CR cells was slightly reduced. Purification via sucrose-gradient led to a greater increase in potency for material produced in perfusion mode compared to batch mode.

In conclusion, evaluation of a series of process conditions in semi-perfusion shake flask and STR batch cultures led to successful implementation of a scalable perfusion HCD process for all three candidate cell lines. This enabled production of rVSV-NDV above  $10^{11}$  infectious virus particles. Using an acoustic settler, the direct harvesting of rVSV-NDV will allow for a seamless integration into downstream processing trains. The influence of HCD conditions, perfusion mode, and syncytia formation during production on the oncolytic potency of rVSV-NDV must still be confirmed in preclinical tumor models. Nevertheless, results clearly represent an important step toward a high-yield manufacturing process for rVSV-NDV and other potential OVs.

## AUTHOR CONTRIBUTIONS

**Sven Göbel:** Conceptualization; methodology; investigation; writing—original draft; writing—review and editing; project administration. **Karim E. Jaén:** Conceptualization; methodology; investigation; writing—original draft; writing—review and editing; project administration. **Yvonne Genzel:** Conceptualization; methodology; writing—review and editing; supervision; project administration. **Udo Reichl:** Conceptualization; writing—review and editing; supervision. **Jennifer Altomonte:** Conceptualization; writing—review and editing; supervision. **Marie Dorn:** Investigation; writing—review and editing. **Victoria Neumeyer:** Investigation; writing—review and editing. **Ingo Jordan:** Writing—review and editing. **Volker Sandig:** Writing—review and editing.

## ACKNOWLEDGMENTS

The authors would like to thank Ilona Behrendt for the excellent technical support, Pavel Marichal Gallardo for his support in the quantification of DNA and protein, and Fabian Kortum and Teresa Krabbe for their participation in fruitful discussions. The help of M. Prömmel and B. Hundt (Ceva Innovation Center GmbH) on the BHK-21 cells is equally acknowledged. Part of the funding for this work was provided by the EXIST-Forschungstransfer program (financed by the Federal Ministry for Economic Affairs and Energy) under the grant agreement #03EFOBY215 awarded to Jennifer Altomonte. Open Access funding enabled and organized by Projekt DEAL.

## CONFLICTS OF INTEREST STATEMENT

Jennifer Altomonte (WO 2017/198779) holds a patent for the development and use of rVSV-NDV as an oncolytic therapy of cancer and is co-founder of Fusix Biotech GmbH, which is developing the rVSV-NDV technology for clinical use. Ingo Jordan and Volker Sandig are employees of ProBioGen AG where AGE1.CR.pIX, and CD-U7 have been developed.

## DATA AVAILABILITY STATEMENT

Data available in article supplementary material. Additional data is available on request from the authors. The data that support the findings of this study are available from the corresponding author, Yvonne Genzel, upon reasonable request.

## ETHICS STATEMENT

This article does not contain any studies with human participants or animals performed by any of the authors.

## ORCID

Marie Dorn  <http://orcid.org/0000-0002-5188-258X>

Ingo Jordan  <http://orcid.org/0000-0003-2711-7252>

Yvonne Genzel  <http://orcid.org/0000-0002-2264-5569>

## REFERENCES

- Abaandou, L., Quan, D., & Shiloach, J. (2021). Affecting HEK293 cell growth and production performance by modifying the expression of specific genes. *Cells*, 10(7), 1667. <https://doi.org/10.3390/cells10071667>
- Abdullahi, S., Jäkel, M., Behrendt, S. J., Steiger, K., Topping, G., Krabbe, T., Colombo, A., Sandig, V., Schiergens, T. S., Thasler, W. E., Werner, J., Lichtenthaler, S. F., Schmid, R. M., Ebert, O., & Altomonte, J. (2018). A novel chimeric oncolytic virus vector for improved safety and efficacy as a platform for the treatment of hepatocellular carcinoma. *Journal of Virology*, 92(23);e01386-18. <https://doi.org/10.1128/jvi.01386-18>
- Adamson, L., & Walum, E. (2007). Insulin and IGF-1 mediated inhibition of apoptosis in CHO cells grown in suspension in a protein-free medium. *Alternatives to Laboratory Animals*, 35(3), 349–352.
- Aunins, J. G. (2003). Viral Vaccine Production in Cell Culture. In R. E. Spier (Ed.), *Encyclopedia of Cell Technology* (p. 12). <https://doi.org/10.1002/0471250570.spi105>
- Bock, A., Schulze-Horsel, J., Schwarzer, J., Rapp, E., Genzel, Y., & Reichl, U. (2011). High-density microcarrier cell cultures for influenza virus production. *Biotechnology Progress*, 27(1), 241–250. <https://doi.org/10.1002/btpr.539>
- Cook, M., & Chauhan, A. (2020). Clinical application of oncolytic viruses: A systematic review. *International Journal of Molecular Sciences*, 21(20), 7505. <https://doi.org/10.3390/ijms21207505>
- Coronel, J., Behrendt, I., Bürgin, T., Anderlei, T., Sandig, V., Reichl, U., & Genzel, Y. (2019). Influenza A virus production in a single-use orbital shaken bioreactor with ATF or TFF perfusion systems. *Vaccine*, 37(47), 7011–7018. <https://doi.org/10.1016/j.vaccine.2019.06.005>
- Coronel, J., Gränicher, G., Sandig, V., Noll, T., Genzel, Y., & Reichl, U. (2020). Application of an inclined settler for cell culture-based influenza A virus production in perfusion mode. *Frontiers in Bioengineering and Biotechnology*, 8, 672. <https://doi.org/10.3389/fbioe.2020.00672>
- Dumont, J., Eewart, D., Mei, B., Estes, S., & Kshirsagar, R. (2016). Human cell lines for biopharmaceutical manufacturing: History, status, and future perspectives. *Critical Reviews in Biotechnology*, 36(6), 1110–1122. <https://doi.org/10.3109/07388551.2015.1084266>
- Eagle, H. (1959). Amino acid metabolism in mammalian cell cultures. *Science*, 130(3373), 432–437.
- Elahi, S. M., Shen, C. F., & Gilbert, R. (2019). Optimization of production of vesicular stomatitis virus (VSV) in suspension serum-free culture medium at high cell density. *Journal of Biotechnology*, 289, 144–149.
- EMA. (2009). *ICH considerations oncolytic viruses*. ((EMA/CHMP/ICH/607698/2008)). [https://www.ema.europa.eu/en/documents/scientific-guideline/international-conference-harmonisation-technical-requirements-registration-pharmaceuticals-human-use\\_en-2.pdf](https://www.ema.europa.eu/en/documents/scientific-guideline/international-conference-harmonisation-technical-requirements-registration-pharmaceuticals-human-use_en-2.pdf)
- Emma, P., & Kamen, A. (2013). Real-time monitoring of influenza virus production kinetics in HEK293 cell cultures. *Biotechnology Progress*, 29(1), 275–284.
- Ferreira, T. B., Carrondo, M. J. T., & Alves, P. M. (2007). Effect of ammonia production on intracellular pH: Consequent effect on adenovirus vector production. *Journal of Biotechnology*, 129(3), 433–438. <https://doi.org/10.1016/j.jbiotec.2007.01.010>
- Fontana, D., Kratje, R., Etcheverrigaray, M., & Prieto, C. (2014). Rabies virus-like particles expressed in HEK293 cells. *Vaccine*, 32(24), 2799–2804.
- Gallo-Ramírez, L. E., Nikolay, A., Genzel, Y., & Reichl, U. (2015). Bioreactor concepts for cell culture-based viral vaccine production. *Expert Review of Vaccines*, 14(9), 1181–1195. <https://doi.org/10.1586/14760584.2015.1067144>
- Gálvez, J., Lecina, M., Solà, C., Cairó, J. J., & Gòdia, F. (2012). Optimization of HEK-293S cell cultures for the production of adenoviral vectors in bioreactors using on-line OUR measurements. *Journal of Biotechnology*, 157(1), 214–222.
- Gauss-Muller, V., & Deinhardt, F. (1984). Effect of hepatitis A virus infection on cell metabolism in vitro. *Experimental Biology and Medicine*, 175(1), 10–15.
- Genzel, Y., & Reichl, U. (2009). Continuous cell lines as a production system for influenza vaccines. *Expert Review of Vaccines*, 8(12), 1681–1692. <https://doi.org/10.1586/erv.09.128>
- Genzel, Y., Vogel, T., Buck, J., Behrendt, I., Ramirez, D. V., Schiedner, G., Jordan, I., & Reichl, U. (2014). High cell density cultivations by alternating tangential flow (ATF) perfusion for influenza A virus production using suspension cells. *Vaccine*, 32(24), 2770–2781. <https://doi.org/10.1016/j.vaccine.2014.02.016>
- Ghafari-Esfahani, A., Shokri, R., Sharifi, A., Shafiee, L., Khosravi, R., Kaghazian, H., & Khalili, M. (2020). Optimization of parameters affecting on CHO cell culture producing recombinant erythropoietin. *Preparative Biochemistry & Biotechnology*, 50(8), 834–841.
- Göbel, S., Kortum, F., Chavez, K. J., Jordan, I., Sandig, V., Reichl, U., & Genzel, Y. (2022). Cell-line screening and process development for a fusogenic oncolytic virus in small-scale suspension cultures. *Applied Microbiology and Biotechnology*, 106(13–16), 4945–4961. <https://doi.org/10.1007/s00253-022-12027-5>

- Göbel, S., Pelz, L., Reichl, U., & Genzel, Y. (2022). Chapter 5 upstream processing for viral vaccines—Process intensification. In L. C. Amine Kamen (Ed.), *Bioprocessing of Viral Vaccines* (Vol. 1, pp. 79–137). Taylor & Francis Group.
- Gränicher, G., Babakhani, M., Göbel, S., Jordan, I., Marichal-Gallardo, P., Genzel, Y., & Reichl, U. (2021). A high cell density perfusion process for modified vaccinia virus Ankara production: Process integration with inline DNA digestion and cost analysis. *Biotechnology and Bioengineering*, 118, 4720–4734. <https://doi.org/10.1002/bit.27937>
- Gränicher, G., Coronel, J., Trampler, F., Jordan, I., Genzel, Y., & Reichl, U. (2020). Performance of an acoustic settler versus a hollow fiber-based ATF technology for influenza virus production in perfusion. *Applied Microbiology and Biotechnology*, 104(11), 4877–4888. <https://doi.org/10.1007/s00253-020-10596-x>
- Grein, T. A., Loewe, D., Dieken, H., Weidner, T., Salzig, D., & Czermak, P. (2019). Aeration and shear stress are critical process parameters for the production of oncolytic measles virus [original research]. *Frontiers in Bioengineering and Biotechnology*, 17(7):78. <https://doi.org/10.3389/fbioe.2019.00078>
- Gripon, P., Diot, C., Corlu, A., & Guguen-Guillouzo, C. (1989). Regulation by dimethylsulfoxide, insulin, and corticosteroids of hepatitis B virus replication in a transfected human hepatoma cell line. *Journal of Medical Virology*, 28(3), 193–199. <https://doi.org/10.1002/jmv.1890280316>
- Hadpe, S. R., Sharma, A. K., Mohite, V. V., & Rathore, A. S. (2017). ATF for cell culture harvest clarification: Mechanistic modelling and comparison with TFF. *Journal of Chemical Technology & Biotechnology*, 92(4), 732–740. <https://doi.org/10.1002/jctb.5165>
- Hein, M. D., Chawla, A., Cattaneo, M., Kupke, S. Y., Genzel, Y., & Reichl, U. (2021). Cell culture-based production of defective interfering influenza A virus particles in perfusion mode using an alternating tangential flow filtration system. *Applied Microbiology and Biotechnology*, 105(19), 7251–7264. <https://doi.org/10.1007/s00253-021-11561-y>
- Hein, M. D., Kollmus, H., Marichal-Gallardo, P., Püttker, S., Benndorf, D., Genzel, Y., & Reichl, U. (2021). OP7, a novel influenza A virus defective interfering particle: Production, purification, and animal experiments demonstrating antiviral potential. *Applied Microbiology and Biotechnology*, 105(1), 129–146. <https://doi.org/10.1007/s00253-020-11029-5>
- Henry, O., Dormond, E., Perrier, M., & Kamen, A. (2004). Insights into adenoviral vector production kinetics in acoustic filter-based perfusion cultures. *Biotechnology and Bioengineering*, 86(7), 765–774. <https://doi.org/10.1002/bit.20074>
- Ho, Y. Y., Lu, H. K., Lim, Z. F. S., Lim, H. W., Ho, Y. S., & Ng, S. K. (2021). Applications and analysis of hydrolysates in animal cell culture. *Bioresources and Bioprocessing*, 8(1), 93. <https://doi.org/10.1186/s40643-021-00443-w>
- Jordan, I., John, K., Höwing, K., Lohr, V., Penzes, Z., Gubucz-Sombor, E., Fu, Y., Gao, P., Harder, T., Zádori, Z., & Sandig, V. (2016). Continuous cell lines from the Muscovy duck as potential replacement for primary cells in the production of avian vaccines. *Avian Pathology*, 45(2), 137–155. <https://doi.org/10.1080/03079457.2016.1138280>
- Jordan, I., Northoff, S., Thiele, M., Hartmann, S., Horn, D., Höwing, K., Bernhard, H., Oehmke, S., von Horsten, H., Rebeski, D., Hinrichsen, L., Zelnik, V., Mueller, W., & Sandig, V. (2011). A chemically defined production process for highly attenuated poxviruses. *Biologicals*, 39(1), 50–58. <https://doi.org/10.1016/j.biologicals.2010.11.005>
- Kamen, A., & Henry, O. (2004). Development and optimization of an adenovirus production process. *The Journal of Gene Medicine*, 6(S1), S184–S192.
- Kaptein, L., Greijer, A., Valerio, D., & van Beusechem, V. (1997). Optimized conditions for the production of recombinant amphotropic retroviral vector preparations. *Gene Therapy*, 4(2), 172–176. <https://doi.org/10.1038/sj.gt.3300373>
- Klenk, H. D., Rott, R., Orlich, M., & Blödorn, J. (1975). Activation of influenza A viruses by trypsin treatment. *Virology*, 68, 426–439.
- Krabbe, T., & Altomonte, J. (2018). Fusogenic viruses in oncolytic immunotherapy. *Cancers*, 10(7), 216. <https://www.mdpi.com/2072-6694/10/7/216>
- Krabbe, T., Marek, J., Groll, T., Steiger, K., Schmid, R. M., Krackhardt, A. M., & Altomonte, J. (2021). Adoptive T cell therapy is complemented by oncolytic virotherapy with fusogenic VSV-NDV in combination treatment of murine melanoma. *Cancers*, 13(5), 1044. <https://www.mdpi.com/2072-6694/13/5/1044>
- Lavado-García, J., Cervera, L., & Gòdia, F. (2020). An alternative perfusion approach for the intensification of virus-like particle production in HEK293 cultures. *Frontiers in Bioengineering and Biotechnology*, 8, 617. <https://doi.org/10.3389/fbioe.2020.00617>
- Le Ru, A., Jacob, D., Transfiguración, J., Ansonge, S., Henry, O., & Kamen, A. A. (2010). Scalable production of influenza virus in HEK-293 cells for efficient vaccine manufacturing. *Vaccine*, 28(21), 3661–3671. <https://doi.org/10.1016/j.vaccine.2010.03.029>
- Lim, H. S., Chang, K. H., & Kim, J. H. (1999). Effect of oxygen partial pressure on production of animal virus (VSV). *Cytotechnology*, 31(3), 265–270. <https://doi.org/10.1023/A:1008060502532>
- Manceur, A. P., Kim, H., Misisic, V., Andreev, N., Dorion-Thibaudeau, J., Lanthier, S., Bernier, A., Tremblay, S., Gélinas, A. M., Broussau, S., Gilbert, R., & Ansonge, S. (2017). Scalable lentiviral vector production using stable HEK293SF producer cell lines. *Human Gene Therapy Methods*, 28(6), 330–339. <https://doi.org/10.1089/hgtb.2017.086>
- Marichal-Gallardo, P., Pieler, M. M., Wolff, M. W., & Reichl, U. (2017). Steric exclusion chromatography for purification of cell culture-derived influenza A virus using regenerated cellulose membranes and polyethylene glycol. *Journal of Chromatography A*, 1483, 110–119. <https://doi.org/10.1016/j.chroma.2016.12.076>
- Miar, A., Arnaiz, E., Bridges, E., Beedie, S., Cribbs, A. P., Downes, D. J., Beagrie, R. A., Rehwinkel, J., & Harris, A. L. (2020). Hypoxia induces transcriptional and translational downregulation of the type I IFN pathway in multiple cancer cell types. *Cancer Research*, 80(23), 5245–5256. <https://doi.org/10.1158/0008-5472.CAN-19-2306>
- Mounce, B. C., Olsen, M. E., Vignuzzi, M., & Connor, J. H. (2017). Polyamines and their role in virus infection. *Microbiology and Molecular Biology Reviews*, 81(4), e00029–17. <https://doi.org/10.1128/mmr.00029-17>
- Nadeau, I., & Kamen, A. (2003). Production of adenovirus vector for gene therapy. *Biotechnology Advances*, 20(7-8), 475–489.
- Nienow, A. W. (2021). The impact of fluid dynamic stress in stirred bioreactors—the scale of the biological entity: A personal view. *Chemie Ingenieur Technik*, 93(1-2), 17–30.
- Nikolay, A. (2020). *Intensified yellow fever and Zika virus production in animal cell culture*, PhD Thesis, Otto-von-Guericke-Universität, Magdeburg. <https://doi.org/10.25673/33512>
- Nikolay, A., Grooth, J., Genzel, Y., Wood, J. A., & Reichl, U. (2020). Virus harvesting in perfusion culture: Choosing the right type of hollow fiber membrane. *Biotechnology and Bioengineering*, 117(10), 3040–3052. <https://doi.org/10.1002/bit.27470>
- Nikolay, A., Léon, A., Schwamborn, K., Genzel, Y., & Reichl, U. (2018). Process intensification of EB66® cell cultivations leads to high-yield yellow fever and Zika virus production. *Applied Microbiology and Biotechnology*, 102(20), 8725–8737. <https://doi.org/10.1007/s00253-018-9275-z>
- Pelz, L., Göbel, S., Chavez, K., Reichl, U., & Genzel, Y. (2022). Chapter 5 Upstream processing for viral vaccines—General aspects. In L. C. Amine Kamen (Ed.), *Bioprocessing of Viral Vaccines* (Vol. 1, pp. 79–137). Taylor & Francis Group.
- Perrin, P., Madhusudana, S., Gontier-Jallet, C., Petres, S., Tordo, N., & Merten, O.-W. (1995). An experimental rabies vaccine produced with a new BHK-21 suspension cell culture process: Use of

- serum-free medium and perfusion-reactor system. *Vaccine*, 13(13), 1244–1250. [https://doi.org/10.1016/0264-410X\(94\)00022-F](https://doi.org/10.1016/0264-410X(94)00022-F)
- Petiot, E., Cuperlovic-Culf, M., Shen, C. F., & Kamen, A. (2015). Influence of HEK293 metabolism on the production of viral vectors and vaccine. *Vaccine*, 33(44), 5974–5981.
- Petiot, E., Jacob, D., Lanthier, S., Lohr, V., Ansoerge, S., & Kamen, A. A. (2011). Metabolic and kinetic analyses of influenza production in perfusion HEK293 cell culture. *BMC Biotechnology*, 11, 84. <https://doi.org/10.1186/1472-6750-11-84>
- Pihl, A. F., Offersgaard, A. F., Mathiesen, C. K., Prentoe, J., Fahnøe, U., Krarup, H., Bukh, J., & Gottwein, J. M. (2018). High density Huh7.5 cell hollow fiber bioreactor culture for high-yield production of hepatitis C virus and studies of antivirals. *Scientific Reports*, 8(1), 17505. <https://doi.org/10.1038/s41598-018-35010-5>
- Planz, O. (2013). Development of cellular signaling pathway inhibitors as new antivirals against influenza. *Antiviral Research*, 98(3), 457–468.
- Rodrigues, A. F., Formas-Oliveira, A. S., Bandeira, V. S., Alves, P. M., Hu, W. S., & Coroadinha, A. S. (2013). Metabolic pathways recruited in the production of a recombinant enveloped virus: Mining targets for process and cell engineering. *Metabolic Engineering*, 20, 131–145. <https://doi.org/10.1016/j.ymben.2013.10.001>
- Scholtissek, C., Müller, K., & Herzog, S. (1986). Influence of insulin and 12-O-tetradecanoylphorbol-13-acetate (TPA) on influenza virus multiplication. *Virus Research*, 6(3), 287–294.
- Schwarz, H., Zhang, Y., Zhan, C., Malm, M., Field, R., Turner, R., Sellick, C., Varley, P., Rockberg, J., & Chotteau, V. (2020). Small-scale bioreactor supports high density HEK293 cell perfusion culture for the production of recombinant erythropoietin. *Journal of Biotechnology*, 309, 44–52. <https://doi.org/10.1016/j.jbiotec.2019.12.017>
- Seitz, C., Isken, B., Heynisch, B., Rettkowski, M., Frensing, T., & Reichl, U. (2012). Trypsin promotes efficient influenza vaccine production in MDCK cells by interfering with the antiviral host response. *Applied Microbiology and Biotechnology*, 93(2), 601–611. <https://doi.org/10.1007/s00253-011-3569-8>
- Sunstrom, N. A. S., Gay, R. D., Wong, D. C., Kitchen, N. A., DeBoer, L., & Gray, P. P. (2000). Insulin-like growth factor-I and transferrin mediate growth and survival of Chinese hamster ovary cells. *Biotechnology Progress*, 16(5), 698–702.
- Tapia, F., Vázquez-Ramírez, D., Genzel, Y., & Reichl, U. (2016). Bioreactors for high cell density and continuous multi-stage cultivations: Options for process intensification in cell culture-based viral vaccine production. *Applied Microbiology and Biotechnology*, 100(5), 2121–2132.
- Ungerechts, G., Bossow, S., Leuchs, B., Holm, P. S., Rommelaere, J., Coffey, M., Coffin, R., Bell, J., & Nettelbeck, D. M. (2016). Moving oncolytic viruses into the clinic: Clinical-grade production, purification, and characterization of diverse oncolytic viruses. *Molecular Therapy. Methods & Clinical Development*, 3, 16018. <https://doi.org/10.1038/mtm.2016.18>
- Vázquez-Ramírez, D., Genzel, Y., Jordan, I., Sandig, V., & Reichl, U. (2018). High-cell-density cultivations to increase MVA virus production. *Vaccine*, 36(22), 3124–3133.
- Vázquez-Ramírez, D., Jordan, I., Sandig, V., Genzel, Y., & Reichl, U. (2019). High titer MVA and influenza A virus production using a hybrid fed-batch/perfusion strategy with an ATF system. *Applied Microbiology and Biotechnology*, 103(7), 3025–3035.
- Venereo-Sanchez, A., Gilbert, R., Simoneau, M., Caron, A., Chahal, P., Chen, W., Ansoerge, S., Li, X., Henry, O., & Kamen, A. (2016). Hemagglutinin and neuraminidase containing virus-like particles produced in HEK-293 suspension culture: An effective influenza vaccine candidate. *Vaccine*, 34(29), 3371–3380.
- Wechuck, J. B., Ozuer, A., Goins, W. F., Wolfe, D., Oligino, T., Glorioso, J. C., & Atai, M. M. (2002). Effect of temperature, medium composition, and cell passage on production of herpes-based viral vectors. *Biotechnology and Bioengineering*, 79(1), 112–119. <https://doi.org/10.1002/bit.10310>
- Wood, H. A., Johnston, L. B., & Burand, J. P. (1982). Inhibition of *Autographa californica* nuclear polyhedrosis virus replication in high-density *Trichoplusia ni* cell cultures. *Virology*, 119(2), 245–254. [https://doi.org/10.1016/0042-6822\(82\)90085-x](https://doi.org/10.1016/0042-6822(82)90085-x)
- Wu, Y., Bissinger, T., Genzel, Y., Liu, X., Reichl, U., & Tan, W.-S. (2021). High cell density perfusion process for high yield of influenza A virus production using MDCK suspension cells. *Applied Microbiology and Biotechnology*, 105(4), 1421–1434. <https://doi.org/10.1007/s00253-020-11050-8>
- Yuk, I. H. Y., Olsen, M. M., Geyer, S., & Forestell, S. P. (2004). Perfusion cultures of human tumor cells: A scalable production platform for oncolytic adenoviral vectors. *Biotechnology and Bioengineering*, 86(6), 637–642. <https://doi.org/10.1002/bit.20158>

## SUPPORTING INFORMATION

Additional supporting information can be found online in the Supporting Information section at the end of this article.

**How to cite this article:** Göbel, S., Jaén, K. E., Dorn, M., Neumeyer, V., Jordan, I., Sandig, V., Reichl, U., Altomonte, J., & Genzel, Y. (2023). Process intensification strategies toward cell culture-based high-yield production of a fusogenic oncolytic virus. *Biotechnology and Bioengineering*, 120, 2639–2657. <https://doi.org/10.1002/bit.28353>